

Statics and Dynamics of the 10-state mean-field Potts glass model: A Monte Carlo study

Claudio Brangian, Walter Kob* and Kurt Binder
*Institut für Physik, Johannes Gutenberg Universität Mainz, D-55099
 Mainz, Staudinger Weg 7, Germany*

16. June, 2001

Abstract

We investigate by means of Monte Carlo simulations the fully connected p -state Potts model for different system sizes in order to see how the static and dynamic properties of a finite model compare with the, exactly known, behavior of the system in the thermodynamic limit. Using $p = 10$ we are able to study the equilibrium dynamics for system sizes as large as $N = 2560$. We find that the static quantities, such as the energy, the entropy, the spin glass susceptibility as well as the distribution of the order parameter $P(q)$ show very strong finite size effects. From $P(q)$ we calculate the forth order cumulant $g_4(N, T)$ and the Guerra parameter $G(N, T)$ and show that these quantities cannot be used to locate the static transition temperature for the system sizes investigated. Also the spin-autocorrelation function $C(t)$ shows strong finite size effects in that it does not show a plateau even for temperatures around the dynamical critical temperature T_D . We show that the N - and T -dependence of the α -relaxation time can be understood by means of a dynamical finite size scaling Ansatz. $C(t)$ does not obey the time-temperature superposition principle for temperatures around T_D , but does so for significantly lower T . Finally we study the relaxation dynamics of the individual spins and show that their dependence on time depends strongly on the chosen spin, i.e. that the system is dynamically very heterogeneous, which explains the non-exponentiality of $C(t)$.

I. INTRODUCTION

In recent years it has been recognized that the relaxation dynamics of supercooled liquids and the one of spin glass systems have many properties in common [1–4]. Of particular significance was the observation by Kirkpatrick, Thirumalai, and Wolynes [5], that for certain

*Author to whom correspondence should be addressed. Present and permanent address: Laboratoire des Verres, Université Montpellier II, 34095 Montpellier, France

mean field spin glasses the equations of motion for the spin-autocorrelation function $C(t)$ are formally the same as the ones that have been derived previously for the relaxation of particle density correlation functions of structural glasses [6]. That result thus opened the possibility to find one common description for these two classes of glassy systems: The spin glasses with quenched disorder and the structural glasses in which the disorder is not included explicitly in the Hamiltonian.

One of the important classes of spin glasses models is the Potts glass [5,7–19], which is a generalization of the Ising spin glass [20–27], where the spins σ_i can assume two values ($\sigma_i = \pm 1$), to the case where each Potts “spin” can be in one of p discrete states, $\sigma_i \in \{1, 2, \dots, p\}$, p being an integer. Just as the Potts ferromagnet [28–30] is a “workhorse” for the statistical mechanics of phase transitions, since it has served to test many methods and to exemplify many concepts about the subject, one can expect that the Potts glass will play a similar role for the study of the glass transition in systems with quenched disorder or the properties of liquids close to their glass transition temperature, since the possibility to change p allows to describe different glass transition scenarios, e.g. from a continuous transition to a discontinuous one.

It is important to note that in the Potts glass it is well established that for $p > 4$ one has both a *dynamical* transition at a temperature T_D , where the relaxation time associated with $C(t)$ diverges, and a *static* transition at a temperature $T_0 < T_D$, where a glass order parameter appears discontinuously, accompanied by a kink in the entropy (as well as in the internal energy). In contrast to this knowledge, for the structural glass transition the existence of an underlying static transition, although proposed long time ago [31,32], is still an open question [33–38]. Thus a study of Potts glasses should help us to understand also better structural glasses and hence is a welcome addition to the large efforts made to identify which structural features distinguish the solid glass from the liquid from which it was formed [6,33–41].

Besides this interest in the Potts glass as a possible prototype model for the structural glass transition, it can also be considered as a coarse-grained model for orientational glasses [42–44]. Experimentally these systems are created by random dilution of molecular crystals, which has the effect that at low temperatures the quadrupole moments of the molecules freeze in random orientations [42]. If the crystal anisotropy singles out p discrete preferred orientations (e.g. the 4 diagonal directions in a cubic crystal), a Potts glass model with p states may give a qualitatively correct description of the system. And, last but not least, the Potts glass model of course completes our knowledge about the different types of phase transitions and ordered phases that spin glasses can have [22–27], which provides an additional motivation for the large activity in this field [5,7–19],

In this work, we use Monte Carlo simulations to study the Potts glass model. Our goal is to clarify to what extent this interesting and nontrivial mean field behavior which is known exactly in the thermodynamic limit, $N \rightarrow \infty$, can be seen for *finite* N . In addition, we want to elucidate the dynamical behavior of the model in greater detail than has been done so far and thus help to clarify the reasons for non-Debye relaxation in glassy systems.

In the present paper, we shall first define the model and introduce the quantities that will be investigated (Sec. 2). In Sec. 3 we summarize what is known about the static behavior of the model and describes our pertinent numerical results. Sec. 4 is then devoted to the dynamical properties in the high temperature phase, i.e. above T_D , and the finite size

behavior at T_D , while Sec. 5 is concerned with the dynamical behavior of small systems in the low temperature phase. By following the relaxation of individual spins we are able to study also the “dynamical heterogeneities” [45,46] at low temperatures. Sec. 6 finally summarizes our conclusions.

II. MODEL AND SIMULATION METHODS

In this section we define the Hamiltonian and the observables that we consider in this work. Subsequently we give the details on the simulations.

The Hamiltonian of the p -state mean-field Potts glass of N interacting Potts spins σ_i ($i = 1, 2, \dots, N$) that can take p discrete values $\sigma_i \in \{1, 2, \dots, p\}$ is defined as

$$\mathcal{H} = - \sum_{i < j} J_{ij} (p \delta_{\sigma_i \sigma_j} - 1). \quad (1)$$

The “exchange constants” (bonds) J_{ij} are quenched random variables which we assume to be distributed according to a Gaussian distribution $P(J_{ij})$

$$P(J_{ij}) = \frac{1}{\sqrt{2\pi}(\Delta J)} \exp \left[- \frac{(J_{ij} - J_0)^2}{2(\Delta J)^2} \right]. \quad (2)$$

The first two moments J_0 and ΔJ are chosen as follows:

$$J_0 \equiv [J_{ij}]_{av} = \tilde{J}_0 / (N - 1), \quad \tilde{J}_0 = 3 - p, \quad (3)$$

$$(\Delta J)^2 \equiv [J_{ij}^2]_{av} - [J_{ij}]_{av}^2 = 1 / (N - 1), \quad (4)$$

where $[\dots]_{av}$ denotes an average over all realizations of disordered bonds (while thermal equilibrium averages will be denoted as $\langle \dots \rangle$). The scaling of the parameters $J_0, \Delta J$ with N was chosen such as to ensure a sensible thermodynamic limit both for the spin glass transition and for the ferromagnetic transition (which occurs for a certain range of values of \tilde{J}_0). Note that for $p = 2$ Eqs. (1) - (4) simply reduce to the Sherrington-Kirkpatrick (SK) model of a spin glass [21]. We also mention that the term $\sum_{i < j} J_{ij}$ in Eq. (1) is only included

for convenience, since it makes the mean energy of *each system*, i.e. for each realization of the disorder, go to zero for $T \rightarrow \infty$. For the present choice of the parameter ΔJ , the spin glass transition in the replica-symmetric approximation, within which one finds a second-order transition for $p < 6$, occurs at a temperature $T_s = 1$ [7]. (Here and in the following we set Boltzmann’s constant $k_B \equiv 1$). While for some choices of \tilde{J}_0 the system exhibits a transition to a standard ferromagnetic phase at a temperature $T_F > T_s$, for our choice of parameters T_F falls far below T_s and hence ferromagnetic order is of no of interest here [7,11]

There exists in addition a second transition to a different type of spin glass phase (sometimes called “randomly canted ferromagnetic phase”) [7,9], at a transition temperature T_2 which is given by

$$T_2 = (p/2 - 1) / (1 - \tilde{J}_0). \quad (5)$$

For the choice of \tilde{J}_0 given in Eq. (3) one thus finds $T_2 = 1/2$. Hence this choice ensures that at the temperatures of interest in the present study, $T \geq 0.7$, any effect of this second transition on physical observables should be negligible.

For defining observables like the magnetization, the glass order parameter, time-dependent spin autocorrelation functions, etc., it is useful to choose a representation for the spins that takes into account the symmetry between their p possible states. This can be achieved by the so-called “simplex representation” [29,30] in which the p states correspond to $(p-1)$ -dimensional vectors \vec{S}_λ pointing towards the corners of a p -simplex, i.e.

$$\vec{S}_\lambda \cdot \vec{S}_{\lambda'} = (p\delta_{\lambda\lambda'} - 1) \quad \text{with } \lambda, \lambda' = 1, \dots, p. \quad (6)$$

In our study we consider static as well as dynamical observables. Static quantities include the energy per spin,

$$e = [\langle \mathcal{H} \rangle]_{av}/N, \quad (7)$$

the spin glass susceptibility χ_{SG} , and the spin glass order parameter distribution function $P(q)$. For defining a spin glass order parameter, we follow the standard method used for Potts glasses [12,16,19] to consider two replicas α and β of the system, i.e. two systems that have identical bond configurations, and to make for each of them an independent Monte Carlo simulation. The order parameter tensor is then defined as

$$q^{\mu\nu} = \frac{1}{N} \sum_{i=1}^N (\vec{S}_{i,\alpha})^\mu (\vec{S}_{i,\beta})^\nu \quad \mu, \nu = 1, 2, \dots, p-1 \quad (8)$$

In an equilibrium simulation of a finite system with no external fields that couple to odd moments of the order parameter the symmetry is not broken. Hence it is useful to consider the root mean square order parameter q defined as [5,12,16,19]

$$q = \left[\frac{1}{p-1} \sum_{\mu,\nu=1}^{p-1} (q^{\mu\nu})^2 \right]^{1/2} \quad (9)$$

and by calculating a histogram of q , i.e. by taking first the thermal average and then the average over the disorder, one can estimate the above mentioned distribution $P(q)$. The second moment of this distribution is related to the *reduced* spin glass susceptibility $\tilde{\chi}_{SG}$:

$$\tilde{\chi}_{SG} = \frac{N}{p-1} [\langle q^2 \rangle]_{av} = \frac{N}{p-1} \int_0^1 q^2 P(q) dq. \quad (10)$$

(Below we will discuss the relation between $\tilde{\chi}_{SG}$ and the *standard* spin glass susceptibility χ_{SG} , see Eqs. (21) and (26).) If there is a second order transition to a spin glass phase, $\tilde{\chi}_{SG}$ should show a divergence at the critical temperature. Further interesting quantities related to the distribution $P(q)$ are the reduced fourth-order cumulant [12,16,19]

$$g_4(N, T) = \frac{(p-1)^2}{2} \left(1 + \frac{2}{(p-1)^2} - \frac{[\langle q^4 \rangle]_{av}}{[\langle q^2 \rangle]_{av}^2} \right) \quad (11)$$

and a quantity called the Guerra parameter [47]

$$G(N, T) = \frac{[\langle q^2 \rangle^2]_{av} - [\langle q^2 \rangle]_{av}^2}{[\langle q^4 \rangle]_{av} - [\langle q^2 \rangle]_{av}^2}. \quad (12)$$

The reason for introducing these ratios of moment is that they are useful in the context of finite size scaling analyses of phase transitions. They are defined such that for $N = \infty$ they are zero in the disordered phase and nonzero in the ordered phase. In the finite size scaling limit the curves $g_4(T)$, or $G(T)$, for different system sizes N should intersect in a common point at the static phase transition point. In particular, G is a measure for the lack of self-averaging.

To study the dynamical properties of the system, we will mainly focus on the autocorrelation function of the Potts spins,

$$C(t) = \frac{1}{N(p-1)} \sum_{i=1}^N [\langle \vec{S}_i(t') \cdot \vec{S}_i(t' + t) \rangle]_{av} \quad . \quad (13)$$

Note that in thermal equilibrium $C(t)$ depends only on the time difference t , i.e. it is independent of the second argument t' occurring on the right hand side of Eq. (13). In practice, for the Monte Carlo sampling using the Metropolis algorithm [48], the thermal averaging $\langle \dots \rangle$ is a time averaging over the initial times t' .

We have also considered a rotationally invariant order parameter time-displaced correlation function $C_{RI}(t)$ which is defined as

$$C_{RI}(t) = \left[\frac{\langle \tilde{q}(t) \rangle}{\langle \tilde{q}(0) \rangle} \right]_{av} \quad (14)$$

with

$$\tilde{q}(t) = \left[\frac{1}{p-1} \sum_{\mu, \nu=1}^{p-1} (\tilde{q}^{\mu\nu}(t))^2 \right]^{1/2} \quad \text{and} \quad \tilde{q}^{\mu\nu}(t) = \frac{1}{N} \sum_{i=1}^N (\vec{S}_i)^\mu(t) (\vec{S}_i)^\nu(0). \quad (15)$$

Note that $\tilde{q}^{\mu\nu}$ is not the same quantity as $q^{\mu\nu}$ defined in Eq. (8), since the latter involves two replicas α and β . However, for $t \rightarrow \infty$ the thermodynamic averages of the two quantities are the same. This means that in this limit also \tilde{q} and q , from Eq. (9), are the same. Furthermore we mention that the expectation value $\langle \tilde{q}(0) \rangle$ occurring in Eq. (14) is equal to 1, as long as there is no ferromagnetic ordering of the system. It is important to realize that $C_{RI}(t \rightarrow \infty)$ is not zero, if N is finite. This follows immediately from Eq. (15), since for large t the quantity $\tilde{q}^{\mu\nu}(t)$ is of order $1/\sqrt{N}$ and $\tilde{q}(t)$, as finite sum over such quantities, is hence positive and also of order $1/\sqrt{N}$. From Eq. (10) one also concludes that $C_{RI}(t \rightarrow \infty)$ is of order $\sqrt{\chi_{SG}/N}$.

In our simulations, we have investigated 5 different system sizes, $N = 160, 320, 640, 1280$, and 2560. The number of samples used to approximate the quenched average $[\dots]_{av}$ over the bond disorder was 500 for $N = 160$, 200 for $N = 320$, 100 for $N = 640$ and 1280 and between 20 and 50 for $N = 2560$ (depending on temperature). At not too low temperatures, $T \geq 1$, the straightforward Metropolis algorithm was implemented [48], picking spins at

random and choosing randomly an orientation for them as a trial configuration. Depending on the energy difference ΔE between the old configuration and the trial configuration, the trial configuration was always accepted if $\Delta E < 0$, else it was accepted with probability $P = \exp(-\Delta E/T)$. For temperatures $T < 1$ the equilibrium configurations were generated with the “parallel tempering” technique [49–51]. These equilibrium configurations can both be used to study the static properties of the model and as starting configurations to study the usual Metropolis dynamics in equilibrium and thus to calculate $C(t)$, although at very low temperatures the relaxation is so slow that one cannot follow the complete decay of $C(t)$ to zero. The total computing time (in units of single Pentium II processor with 400MHz) used for this study was of the order of 10 years.

III. STATIC PROPERTIES OF THE 10-STATE POTTS GLASS MODEL

In this section we first discuss the analytic results for the static properties of the model in the thermodynamic limit. Subsequently we compare them with the results of the simulations for finite N .

If one calculates the free energy of the model given by Eqs. (1) - (4) with the replica method [20–27], (without allowing for replica symmetry breaking), one obtains, depending on the value of \tilde{J}_0 but independent of p , either a transition to a spin glass phase (where the spin glass order parameter q_0 is nonzero) or to a ferromagnet (with a spontaneous magnetization m_0). Within this approach and close to a critical temperature T_s the free energy density $f(q_0, m_0)$ can be written as follows [7],

$$-f(q_0, m_0)/T = \frac{1}{2}r' \left(1 - \frac{T_s}{T}\right) q_0^2 + \frac{1}{6}uq_0^3 + \frac{1}{2}r_m m_0^2 + \frac{1}{6}u_m m_0^4 + \frac{1}{6}u' q_0^2 m_0^2 + \dots \quad (16)$$

where with our choice of units $T_s = 1$, and r' , u , r_m , u_m , u' are constants that are of no interest to us here. If the parameters are chosen such that the transition that occurs at T_s is to a spin glass phase, it is found that the order parameter distribution $P(q)$ is a δ -function whose position depends on T (we consider here only the case $u > 0$):

$$P(q) = \delta(q), \quad \text{for } T > T_s \quad (17)$$

$$P(q) = \delta(q - q_0), \quad \text{with } q_0 = \frac{2r'}{u} \left(\frac{T_s}{T} - 1\right), \quad \text{for } T < T_s. \quad (18)$$

Note that the first term on the right hand side of Eq. (16) can also be interpreted in terms of the spin glass susceptibility χ_{SG} as $\frac{1}{4}\chi_{SG}^{-1}q_0^2$ ¹. Thus close to T_s one finds for χ_{SG} a Curie-Weiss law:

$$\chi_{SG} = [2r'(1 - T_s/T)]^{-1}, \quad T > T_s. \quad (19)$$

¹For the definition of a proper conjugate field to define the spin glass susceptibility, see references [22,61]

The coefficient r' in Eq. (16) is given by [7] (a result coming from the expansion in q of the free energy close to T_s)

$$r' = \frac{p-1}{2} \left(\frac{T_s}{T} \right)^2 \left(1 + \frac{T_s}{T} \right). \quad (20)$$

We thus find for the susceptibility χ_{SG} around T_s (remember $T_s = 1$ in our normalization):

$$\chi_{SG}^{-1} = 2(p-1) \left(1 - \frac{T_s}{T} \right), \quad T \approx T_s. \quad (21)$$

The difference between the standard spin glass susceptibility and the reduced one defined in Eq. (10) is just the factor $(p-1)$, related to the susceptibility of a system of non-interacting spins.

It is well known [5,9,11] that, if one allows for replica symmetry breaking, the prediction that there is a second order transition to a spin glass phase remains valid only if $p \leq 4$. For $p > 4$, a new type of first-order transition to a glass phase is predicted to occur at a temperature T_0 which is higher than T_s . Although at T_0 the order parameter jumps discontinuously from zero to a value $q_0 > 0$ there is no latent heat involved in this transition. Instead of Eq. (18) the order parameter distribution acquires now a double- δ function structure [5,9,11],

$$P(q) = [1 - w(T)]\delta(q) + w(T)\delta(q - q_0(T)), \quad T < T_0. \quad (22)$$

with $w(T) = 1 - T/T_0$ for $T \rightarrow T_0^-$. While it is possible to calculate q_0 and T_0 analytically for $p \rightarrow 4^+$, see e.g. [11],

$$q_0 = \frac{2}{7}(p-4) + o(p-4)^2, \quad T_0 - T_s \propto (p-4)^2 + o(p-4)^3, \quad (23)$$

for integer $p > 4$ the correct values for q_0 and T_0 can be obtained only numerically [13]. E.g., for our case of $p = 10$ the predicted values are

$$T_0 = 1.1312 \quad \text{and} \quad q_0(T_0) = 0.452 \quad . \quad (24)$$

In the disordered phase, the internal energy per spin e and entropy per spin s are given by [7,13]

$$e = -\frac{p-1}{2} \frac{T_s}{T}, \quad s = \ln p - \frac{p-1}{4} \left(\frac{T_s}{T} \right)^2. \quad (25)$$

and a high temperature expansion gives [24]

$$\tilde{\chi}_{SG}^{-1} = \left[1 - \left(\frac{T_s}{T} \right)^2 \right], \quad T > T_0. \quad (26)$$

Within the replica symmetric Ansatz these expressions are correct for $T > T_s$. If one allows for replica symmetry breaking they hold only for $T > T_0$. Although no *explicit* analytic expression for $e(T)$ and $s(T)$ are known for $T < T_0$ their value can be calculated numerically [13].

Finally we mention that within the replica Ansatz (symmetric or broken) neither T_s nor T_0 depend on the choice of \tilde{J}_0 from Eq. (3), provided that the transition temperature T_F from the disordered phase to the collinear ferromagnetic phase, discussed in section II, is not above T_0 [7,11]. T_F is given by the following equation, for arbitrary p [7]

$$T_F^{-1} = \frac{\tilde{J}_0}{(p-2)} \left[-1 + \sqrt{1 + 2(p-2)/\tilde{J}_0^2} \right] \quad (27)$$

DeSantis *et al.* [13] used $\tilde{J}_0 = \frac{1}{2}(4-p)$ in which case $T_F = T_s = 1$, independent of p . However, this case is rather special since then the transition temperature T_2 to the randomly canted ferromagnetic phase, discussed in the Introduction, coincides with $T_s = 1$, as can be seen from Eq. (5). For our choice of $\tilde{J}_0 = 3-p$ we have instead $T_2 = 1/2$ for all p and $T_F = 8/(7 - \sqrt{65}) \approx 0.531$ for $p = 10$. Thus with this choice we hence make sure that the ferromagnetic fluctuations are still very small at $T_s = 1$, even if the system size is rather small.

We now present our numerical results and compare them to the analytical predictions that we just discussed. Fig. 1a shows a plot of the internal energy versus inverse temperature, over a wide temperature range ($0.7 \leq T \leq 2$), but still clearly above the temperatures T_F and T_2 (remember that $\beta_F \equiv 1/T_F \approx 1.88$, $\beta_2 \equiv 1/T_2 = 2.0$). Also included are the theoretical predictions for $N \rightarrow \infty$ obtained within the replica symmetric and one-step replica symmetry breaking theory, respectively. This figure reveals unexpectedly large finite size effects over a broad temperature regime in that, e.g., the energy for $N = 640$ coincides with the asymptotic result only if $\beta \lesssim 0.6$. For $\beta \gtrsim 0.6$ clear deviations from the asymptotic solution are visible, which are larger for smaller N . The numerical data for finite N , in the range accessible to our work, reveal only a smooth crossover from the regime of the disordered high temperature phase to the regime of the low temperature glass-like phase, and no indication of the kink at β_0 , predicted by the one-step replica symmetry breaking theory, is yet visible. As expected even for $N \rightarrow \infty$, there is no effect of the dynamical transition at $\beta_D \equiv 1/T_D$ on static quantities like the energy.

Of course it is also of interest to study how at fixed temperature the energy $e_N(T)$ converges to its asymptotic limit $e_\infty(T)$. Fig. 1b shows that the energy difference $e_N(T) - e_\infty(T)$ scales like N^{-1} both for temperatures above the static transition temperature T_0 and for temperatures below T_0 , while at T_0 a different law, ($\propto N^{-2/3}$), seems to hold (see inset). (Note that we plot here data for T_D instead of T_0 since we have simulated more system sizes at this temperature. However, since the two temperatures are so close to each other this difference should not matter for the system sizes investigated here.)

We have also calculated the temperature dependence of the entropy $s(T)$. This was done by a thermodynamic integration [52] of the free energy f :

$$s(\beta) = \beta e(\beta) - \bar{\beta} f(\bar{\beta}) + \int_{\bar{\beta}}^{\beta} e(\beta) d\beta \quad . \quad (28)$$

We have used $\bar{\beta} = 0.5$, a temperature at which our data is no longer sensitive to finite size effects and thus the replica solution is valid, so that we can use for the free energy $\bar{\beta} f(\bar{\beta}) = \beta e(\bar{\beta}) - s(\bar{\beta})$ the mean-field value $-9/16 - \log(10)$ (see Eq. (25)). The integral over e was done by using a spline interpolation of our data, with 180 points for $N = 160$,

320, 640 and 100 points for $N=1280, 2560$. We think that alternative methods to calculate $e(T)$, such as re-weighting techniques or methods to directly sample the density of states [48], would not bring a significant advantage in our case. The results are shown in Fig. 1c from which we recognize that $s(T)$ shows similar finite size effects as the energy $e(T)$.

From Eq. (25) we see that the entropy at the static transition is

$$s(T_0) = \ln 10 - \frac{9}{4}(T_s/T_0)^2 \approx 0.544, \quad \text{i.e. } s(T_0)/s(T = \infty) \approx 0.236. \quad (29)$$

Thus we see that, while at the static transition temperature T_0 the entropy has decreased to less than a quarter of its high temperature value, it is clearly nonzero (and nonnegative, of course). In supercooled liquids one often extrapolates the temperature dependence of the entropy (minus the vibrational entropy of the crystal) to zero and uses this to define the Kauzmann temperature T_K [31]. If one proceeds in the same way with the current model to obtain a “Kauzmann temperature” T_K where the entropy of the metastable high temperature phase vanishes, one obtains from Eq. (25)

$$T_K/T_s = \frac{3}{2}(\ln 10)^{-1/2} \approx 0.9885 \quad (30)$$

which is even below the “true” metastability limit $T_s = 1$ of the disordered phase, where the (extrapolated) static glass susceptibility is divergent. (Note that the proximity of T_K and T_s happens accidentally for $p = 10$. E.g. for $p = 5$ the general result [7] $T_K/T_s = [\frac{1}{4}(p-1)/\ln p]^{1/2}$ implies $T_K/T_s \approx 0.7882$.) Also a strictly linear extrapolation of $s(T)$ from T_s or T_0 down to a temperature where this extrapolation would vanish does not give a meaningful result, of course.

These results show that the idea to locate the static glass transition temperature by an extrapolation of the (configurational) entropy function $s(T)$ in the disordered high temperature phase to $s(T = T_K) = 0$ [31,32] can be completely misleading, even for a mean-field model that does indeed exhibit both a dynamical transition (at T_D) and a static transition (at T_0). While T_K is always lower than T_0 , it does not coincide with the stability limit of the metastable high temperature phase, and thus lacks any physical significance. Since for the case of polymers theories were formulated that suggest that T_K is the static glass transition temperature [32], it is interesting to note that a simulation study of the glass transition in the framework of the bond fluctuation model found a decrease of s from its high temperature value to about 1/4 of this value, when T is lowered, but that subsequently the curve $s(T)$ vs. T bends over and a well-defined T_k does not exist [54]. The “configurational entropy” estimated by Gibbs and DiMarzio [32] was simply the total entropy of their lattice model of polymers, just as the total entropy of our model shown in Fig. 1b. Thus this demonstrates that the calculation of T_K in this way is most likely wrong. Of course, this “naive” way to define the Kauzmann temperature via the vanishing of the (configurational) entropy $s(T)$ should not be confused with the approach of defining a “complexity” [5,22–27,69]. In that approach one determines the number of basins in the *free* energy and defines T_K as that temperature at which this number starts to become exponentially large.

Fig. 2 shows the reduced spin glass susceptibility as a function of the squared inverse temperature. This representation is adapted to the theoretical temperature dependence of this quantity, see Eq. (26), which predicts at T^{-2} -law at high temperatures. As expected

already from the behavior of the internal energy, even far above T_s and T_0 the convergence to the thermodynamic limit is rather slow. Unfortunately the analysis of the finite size behavior of $\tilde{\chi}_{SG}$ is not straightforward, as we will show in the following. For $T < T_0$ and $N \rightarrow \infty$ Eqs. (10) and (22) imply

$$\tilde{\chi}_{SG}^{-1} = \frac{p-1}{Nq_0^2} \frac{1}{(1-T/T_0)}, \quad (31)$$

since for $T < T_0$ our definition for $\tilde{\chi}_{SG}$, Eq. (10), simply picks up a contribution due to the nonzero spin glass order parameter q_0 . As a result, $\tilde{\chi}_{SG}^{-1}$ for $N \rightarrow \infty$ should follow the straight dashed line in Fig. 2 that represents the replica-symmetric solution for all $T^{-2} < T_0^{-2}$, while for $T^{-2} > T_0^{-2}$, $\tilde{\chi}_{SG}^{-1}$ simply converges towards the abscissa. This singular behavior of $\tilde{\chi}_{SG}^{-1}$ is explained further in the inset, where we have added to $\tilde{\chi}_{SG}^{-1}$ the term $(T_s/T)^2$. This sum gives unity for $T > T_0$ and $(T_s/T)^2$ for $T < T_0$, as can be seen from Eq. (26). For very large but finite N , $\tilde{\chi}_{SG}^{-1}$ for $T < T_0$ exhibits a Curie-Weiss type divergence at T_0 , but the amplitude of this effect is only of order $1/N$, as can be seen from Eq. (31). In order to analyze the finite size rounding of this singularity, one must consider that for N finite the δ -functions in Eq. (22) are broadened into peaks of finite height and nonzero width². Our simulation results for $P(q)$, see Fig. 3, do indeed give evidence that a second peak at $q_0 \neq 0$ develops, distinct from the peak at small q that exists also in the high temperature phase. However, the statistical accuracy of $P(q)$ is not very high due to the well known fact that in the ordered phase this quantity is not self-averaging [22–27], and the number of realizations of the random couplings that we were able to study is insufficient to overcome this problem. Hence we are currently not able to do a proper analysis of the finite size effects of $P(q)$, see Fig. 3b, and thus cannot make a finite size analysis of $\tilde{\chi}_{SG}$.

From Fig 3a we see that even in the high temperature phase, i.e. $T > T_0$, we see a peak in $P(q)$ at a *finite* value of q . That this is, however, a finite size effect is demonstrated in Figs. 3b and 3c where we plot $P(q)$ for different system sizes and show the first moment of $P(q)$ as a function of N , respectively. We see that for temperatures well above T_0 the first moment vanishes like $N^{-1/2}$. However, close to T_0 this type of extrapolation would give a *finite* value of the moment. If instead an extrapolation with $N^{-1/3}$ is done, see inset, one finds again as expected that the moment vanishes. Note that for the second moment of $P(q)$ we would have at $T = T_0$ again a scaling of the type $N^{-2/3}$, as we found for the case of the energy. It is interesting to note that Parisi *et al.* [70], making use of replica symmetry breaking scheme, were able to calculate the finite size scaling exponents for the Ising spin glass, and obtained that $[\langle q^k \rangle]$ scales like $N^{-k/3}$ at the critical temperature (consequently one has that e scales like $N^{-2/3}$). It is thus possible that the same kind of scaling holds also for the Potts glass, although one has to keep in mind that both the nature of the transition and of the replica symmetry breaking pattern is different.

While the results shown so far demonstrate a rather encouraging qualitative consistency between the theoretical predictions and the numerical data, our results for the fourth order

²A phenomenological attempt to describe the finite size behavior for the glass transition of Potts models has been made in [16], but this approach is not followed up here, since it is not consistent with Eq. (22) in the limit to $N \rightarrow \infty$.

cumulant g_4 , Eq. (11), and the Guerra parameter G , Eq. (12), are clearly rather worrisome (Fig. 4). It is seen that the three curves for $g_4(N, T)$ have a rather well-defined common intersection point at $T \approx 1.31$, and the three curves for $G(N, T)$ have a rather well-defined common intersection point at $T \approx 1.24$. Motivated by the standard knowledge and experience with finite size scaling at second order [48,55] and first order [48,56] phase transitions, such intersection points are commonly taken as estimates of the transition temperature [22–27]. However, comparison with the exact result for T_0 , Eq. (24), shows that these intersection points are spurious, and hence cannot be taken as accurate estimates of T_0 . This already is obvious from the data alone, because the two quoted temperatures are not in mutual agreement. We think that in reality neither the three curves for $g_4(N, T)$ nor those for $G(N, T)$ intersect at a unique temperature. Given the relatively large error bars of the data, they only can define temperature intervals ΔT_{g_4} , ΔT_G , in which the three intersection points fall. As $N \rightarrow \infty$, presumably all temperatures of these intersections converge (slowly!) towards T_0 . Since T_0 falls distinctly outside the above intervals, this method of searching for intersection points, which is so successful for locating phase transitions in pure systems [48,55,56], is a complete failure here. We emphasize this problem so strongly, because such techniques are commonly used for studying phase transitions in systems with quenched disorder [27]. Again we stress that an analytical guidance for the description of the finite size rounding of first order glass transitions would be very useful.

IV. DYNAMICAL PROPERTIES IN THE HIGH TEMPERATURE PHASE

In this section we briefly review the theoretical predictions for the relaxation dynamics of the spins. Subsequently we compare these predictions with the results from the simulations.

The theoretical results of Kirkpatrick *et al.* show that the Potts glass with $p > 4$ states has a “dynamical transition” at a temperature $T_D > T_0$, where non-ergodicity sets in [5]. For $T \leq T_D$, the spin correlation function $C(t)$, defined in Eq. (13), no longer decays to zero but gets stuck for $t \rightarrow \infty$ at a nonzero value $q_{EA}(T)$, with [13]

$$T_D = 1.142, \quad q_{EA}(T = T_D) = 0.328 \quad . \quad (32)$$

The details of this transition from ergodic (for $T > T_D$ where $C(t \rightarrow \infty) = 0$) to non-ergodic behavior (for $T < T_D$), as well as the time dependence of $C(t)$ for temperatures around T_D are in fact described by equations [5] formally analogous to equations proposed for the structural glass transition by idealized mode-coupling theory [6]. The qualitative behavior of various quantities expected for $N \rightarrow \infty$ is sketched in Fig. 5. Note that for $T > T_D$ and $T < T_0$ we have $q_0 = q_{EA}$. In the temperature range $T_0 < T < T_D$ we have, however $q_0 = 0$ and $q_{EA} > 0$.

In Fig. 6a we show the time dependence for the spin auto-correlation function $C(t)$ for $N = 1280$ and all temperatures investigated. Here and in the following we will measure time in units of Monte Carlo Steps (MCS), i.e. the average number of updates per spin. Surprisingly we see that even for this rather large system size there is not yet any clear evidence for the development of a plateau for temperatures around T_D . Note that in the thermodynamic limit this function should at $T = T_D$ decay to q_{EA} , i.e. the horizontal line. In contrast to this our system with a finite size is always ergodic, since the free energy barriers

separating the various “valleys” in phase space remain finite at all nonzero temperature. Of course every finite system with no hard-core interactions is in principle ergodic. However, e.g. in structural glasses it is found that even a few hundred particles are sufficient to show a pronounced (effective) ergodic to non-ergodic transition. Thus it is rather astonishing that for the present model the finite size effects are so strong that even for $N = 1280$ and at $T = T_D$ the existence of a plateau can hardly be seen.

Also the time dependence of $C_{RI}(t)$, Eq. (14), shows strong finite size effects, as can be seen from Fig. 6b. We see that, contrary to naive expectation, the long time limit of $C_{RI}(t)$ is not zero but a finite constant. This constant depends on temperature and below we will discuss its origin and its dependence on system size in more detail. At any rate, we see that also this correlation function does not show a plateau even if T is close to T_D and hence we conclude that also $C_{RI}(t)$ converges only very slowly to its behavior in the thermodynamic limit.

In order to discuss the system size dependence of the correlation functions in more detail we show in Fig. 7 $C(t)$ and $C_{RI}(t)$ for different systems sizes and two temperatures. From Fig. 7a we see that, at high temperatures, $C(t)$ shows basically no system size dependence. For low T , however, the relaxation becomes quickly slower with increasing system size and also the shape of the curve changes noticeably. But even at the largest system sizes accessible at this temperature we are not able to see a clear two step relaxation as one would expect for a sufficiently large *but finite* system.

The N -dependence is different in the case of $C_{RI}(t)$, Fig. 7b. Here we see that even at high temperatures the correlation function depends on the system size. This is in agreement with the arguments given in the context of Eq. (14) that $C_{RI}(t \rightarrow \infty)$ should scale like $1/\sqrt{N}$. That one actually find this size dependence is shown in the inset of Fig. 7b. Instead of studying the function $C_{RI}(t)$ one could of course try to consider the reduced normalized function $\phi(t) = [C_{RI}(t) - C_{RI}(t \rightarrow \infty)]/[C_{RI}(0) - C_{RI}(t \rightarrow \infty)]$. However, also this type of correlation function has its problems since on one hand the final asymptote $C_{RI}(t \rightarrow \infty)$ is only known to within a certain statistical error, and on the other hand it shows finite size effects at high temperatures at *short* times, i.e. where $C_{RI}(t)$ is independent of N . In view of these problems with $C_{RI}(t)$ we will in the following focus on $C(t)$ only. However, this is not a serious restriction, since in the thermodynamic limit these two functions should show at low temperatures the same time dependence anyway. That this is indeed the case for the simulations can be inferred from Fig. 7c where we show a parametric plot of $C_{RI}(t)$ versus $C(t)$ at T_D . We see that with increasing system size the curves do approach the diagonal, as expected.

We now address the temperature and N dependence of the relaxation time τ of the system. One possibility to define τ is

$$C(t = \tau) = 0.2. \quad (33)$$

Note that although the value 0.2 is somewhat arbitrary, it is a reasonable choice. The only important thing is that it is significantly less than the height of the plateau in the thermodynamic limit, $q_{EA}(T = T_D)$, cf. Eq. (32). (If we would define a time τ' as $C(t = \tau') = 0.5$, on the other hand, τ' would be finite also below T_D , and even below T_0 , until $q_{EA}(T)$ has increased up to $q_{EA} = 0.5$, due to the temperature dependence of the order parameter, see Fig. 5a.)

Since for $N \rightarrow \infty$ the dynamics of the model should be described by (idealized) mode-coupling theory [5], we expect that $\tau(T)$ shows a power law divergence at T_D [6],

$$\tau \propto (T/T_D - 1)^{-\Delta}, \quad N \rightarrow \infty, \quad (34)$$

where Δ is an exponent which is non-universal (i.e. model dependent), but typically not very different from $\Delta \approx 2$. In order to test the validity of Eq. (34), one can plot $\tau^{-1/\Delta}$ for a reasonable trial value of Δ and look whether the data are compatible with a straight line over a reasonable range of temperature. If this is the case the extrapolation to $\tau^{-1/\Delta} = 0$ should give an estimate for T_D . Fig. 8 shows that for $\Delta = 2.0$ the data is indeed rectified for $1.1 \leq T \leq 1.4$, while outside of this temperature range the curves bend. Since plots for other reasonable choices of Δ look quite similar, the value of Δ can be estimated only within ± 0.5 . In all cases it is difficult to use the estimates for T_D for finite N to extrapolate to the value of T_D in the thermodynamic limit since the N -dependence is rather weak and the error bars of $T_D(N)$ are, due to the mentioned extrapolation, quite substantial. For the case of $\Delta = 2.0$ a dependence of the form $T_D(N) - T_D(\infty) \propto 1/N$ seems, however, to be compatible with the data [51].

In order to provide a more systematic way of extrapolating the relaxation times to the thermodynamic limit, we assume that the dynamical finite size scaling hypothesis [55,58,59] holds and make the Ansatz:

$$\tau = N^{z^*} \tilde{\tau} \{N(T/T_D - 1)^{\Delta/z^*}\} \text{ for } N \rightarrow \infty \text{ and } (T/T_D - 1) \rightarrow 0. \quad (35)$$

The scaling function $\tilde{\tau}(\zeta)$ must obey $\tilde{\tau}(\zeta \rightarrow \infty) \propto \zeta^{-z^*}$ to recover the proper thermodynamic limit, i.e. Eq. (34). Using z^* as a fit parameter (Δ is fixed to 2.0), we thus can try to generate a master curve from the $\tau(T)$ curves for the different system sizes N . That this is indeed possible if one chooses $z^* = 1.5$ is shown in Fig. 9. From this figure we see that for large arguments the master curve does indeed show the expected power-law with an exponent $-z^*$ (dashed line). For $T = T_D$ the argument of $\tilde{\tau}$ vanishes and hence we expect a N -dependence of τ of the form $\tau \propto N^{z^*}$ and the inset of Fig. 9 shows that this is indeed the case.

We mention that Eq. (35) has a well-based theoretical foundation for second order phase transitions [22,55,58,59], i.e. the case in which in Fig. 5 the temperatures T_0 , T_D , and T_s coincide at a unique critical temperature T_c . The diverging relaxation time is then an immediate consequence of a diverging static susceptibility, and dynamic finite size scaling is a consequence of ordinary dynamic scaling [59]. E.g., for second order transitions of mean-field spin glass models one has Eq. (35) with $\Delta/z^* = \gamma_{MF} + 2\beta_{MF} = 3$, since the static mean field exponents of the spin glass order parameter and susceptibility are $\beta_{MF} = 1$ and $\gamma_{MF} = 1$, respectively [22]. Using the value of $\Delta = 2$ [22], one hence finds for z^* the value $2/3$. This result could be expected since the standard finite size scaling result for the critical relaxation in spin glasses *with short range interactions* is $\tau \propto L^z$ with $z = 4$ in the mean field approximation [22]. (Here L is the linear dimension of the system.) This result can now be translated into the behavior of infinite range models at the marginal dimension $d^* = 6$, i.e. at the dimension where mean field theory becomes valid, via $N = L^{d^*}$, which yields $\tau \propto N^{z/d^*} = N^{z^*}$, i.e. $z^* = z/d^* = 2/3$. This result is also compatible with numerical simulations [60]. However, the value $z^* \approx 1.5$ found for the present model is clearly rather unusual and we are not aware of any analytical estimates for this exponent.

A further interesting question concerns the asymptotic decay of the correlation function $C(t)$ towards q_{EA} as $t \rightarrow \infty$ at $T = T_D$. In the context of the structural glass transition the time regime during which the correlation functions are close to the plateau is called the “ β -relaxation” whereas the decay below the plateau is called the “ α -relaxation” [6]. Mode-coupling theory predicts that at T_D the approach to the plateau is given by a power law, i.e.

$$C(t) - q_{EA} \propto t^{-a}, \quad T = T_D. \quad (36)$$

A naive way to check for the presence of such a power law is to make a log-log plot of $C(t) - q_{EA}$ versus time. Fig. 10 shows such a plot for two relatively large systems (curves with open symbols) and we see immediately that there is no straight line, i.e. no power law dependence. However, one must recall that $C(t)$ shows a significant dependence on N and that the prediction of Eq. (36) seems to hold only for systems much larger than the ones studied here. Therefore we have tried to make an extrapolation, keeping time fixed, of the curves for finite N to determine the curve for $N = \infty$. One possibility for such an extrapolation is to plot $C(t, N)$ vs. $1/N$. While such a graph gives a straight line for $N \geq 480$, for smaller N a curvature is clearly apparent. Therefore we tried whether a plot of $C(t, N)$ vs. $\exp(-\text{const} \cdot N)$, where the constant is a fit parameter, gives a straight line and found that for a broad range of times (from $t = 10$ to $t = 300$) this is indeed possible if the constant is approximately $1/400$ [51].

In Fig. 10 we have included the results of these two extrapolations also and we see that they do not give the same result. Since *a priori* it is not clear which type of extrapolation (if any!) is the correct one, it is difficult to tell what the shape of $C(t)$ in the thermodynamic limit really is. It is very interesting to note, however, that the extrapolation with the $1/N$ dependence gives a curve $C(t, N = \infty)$ which is very well compatible with a power law of the form given by Eq. (36). Thus this gives some evidence that the extrapolation with $1/N$ is the correct one. The value for the exponent a we read off is 0.33 ± 0.04 .

It is also interesting to note that the theory predicts a one-to-one correspondence between the value of a and the exponent Δ from Eq. (34) [6]. For a given value of a one can use

$$\frac{\Gamma^2(1+b)}{\Gamma(1+2b)} = \frac{\Gamma^2(1-a)}{\Gamma(1-2a)} \quad (37)$$

to calculate b . (Here $\Gamma(x)$ is the usual Γ -function.). The value of Δ is then given by $1/2a + 1/2b$. If one uses the value $\Delta = 2.0$ and the above relations one finds $a = 0.36$, in very good agreement with the value determined from Fig. 10.

Two other important results from mode-coupling theory concern the shape of the correlators close to T_D in the α -relaxation regime, i.e. in the time window where they fall under the plateau. The theory predicts that in this time regime the correlators can be approximated well with the Kohlrausch-Williams-Watts function, $\exp(-(t/\tau)^\beta)$, a functional form that has been found to work very well in many glassy systems [6,33,35,39]. We find, however, that even close to T_D and the largest systems used, this functional form does not give a good fit to the data.

The second prediction of the theory concerning the α -relaxation is the so-called time-temperature superposition principle. This principle implies that the correlator $C(t)$ can be written as

$$C(t, T) = \tilde{C}(t/\tau(T)), \quad (38)$$

where $\tilde{C}(x)$ is a temperature independent scaling function. The validity of Eq. (38) can be checked if one plots $C(t, T)$ versus $x = t/\tau(T)$. If the superposition principle is valid the curves for the different temperature should fall on a master curve for $x \approx 1$ and large x . For very small values of x , i.e. in the early β -regime, no master curve is expected, since Eq. (38) is supposed to hold only in the α -regime. Fig. 11 shows this kind of scaling plot and we see that even for a rather large system, $N = 1280$, there is no indication of such a time-temperature position principle. Of course, it is possible that this failure to verify Eq. (38) is simply due to finite-size effects. Thus, it would be desirable to check Eq. (38) for much larger systems. However, in view of the strong size effects on the relaxation time τ near and below T_D , see Fig. 13 below, this is impossible for us with the present computer resources.

Although we have just seen that the time-temperature superposition principle does not hold close to T_D *for the accessible system sizes* it is interesting to see whether this is the case also at lower temperatures. For $N = 160$ we have been able to go to temperatures as low as $T = 0.7$ and in Fig. 12 we show the correlator as a function of t/τ . If the curves for all temperatures are considered one finds that the superposition principle does again not hold (main figure). However, if one uses only the curves for the lowest temperatures, see inset, one finds that they all collapse onto a nice master curve. Thus we conclude that at sufficiently low temperatures the time-temperature superposition principle does indeed hold. We mention also, that the shape of this master curve is *not* an exponential, but that a stretched exponential with an exponent around 0.43 gives a satisfactory fit.

In order to be able to understand this result a bit better, one needs to understand in more detail the relaxation of our model for $T < T_D$ and finite N , where all free energy barriers in phase space must obviously be still finite. One could argue that at low temperature the largest barrier dominates the dynamics and hence the relaxation depends on temperature only via a temperature dependent prefactor. This temperature dependence would have to be Arrhenius like and in order to check this we show in Fig. 13 the T -dependence of τ for the different system sizes.

From this figure we see that at the lowest temperatures the T -dependence of τ for the smallest system is indeed Arrhenius like. For temperatures around T_D and higher, one sees however significant deviation from this type of temperature dependence. Also for $N = 320$ one can see at the lowest temperature an Arrhenius law, but the activation energy is significantly larger than the one for $N = 160$. Since for increasing system size the lowest accessible temperature becomes higher and higher, it is not possible to see anymore the crossover from the non-Arrhenius T -dependence at intermediate temperatures to the Arrhenius dependence at small T . But the plot clearly shows that at T_D the relaxation times increases quickly with increasing system size, in agreement with the result from Fig. 9 (inset). Due to our present inability to equilibrate larger systems also significantly below T_D , we cannot determine reliably the N -dependence of the activation energy of the Arrhenius law found at low temperatures. We mention that MacKenzie and Young found for the Sherrington-Kirkpatrick model, i.e. the mean-field Potts glass for $p = 2$, that for small systems ($N \leq 128$) and low temperature ($T = 0.6T_D = 0.6T_s$) the relaxation times increase like $\tau(N) \propto \exp(const \cdot N^{0.5})$ [62] whereas in a recent paper Billoire and Marinari [63] give evidence that the exponent of the power law is $1/3$. If we consider a low temperature,

$T = 0.7$, this type of N -dependence of τ is compatible with our data with an exponent 0.5. However, if we determine the N -dependence of the activation energy in the temperature regime where $\tau(T, N)$ shows an Arrhenius law, we find that this energy increases only very slowly, i.e. like $\log(N)$ or a power of N with a small exponent ($\approx 0.1 = 1/p$). (Note that the reason for the two different N -dependencies is related to the fact that the prefactor of the Arrhenius law depends on N also.)

Fig. 13 shows clearly that for small systems, $N = 160, 320$, and 640 , it is possible to explore the region of temperatures below both the dynamical as well as the static transition. Note that in simulations of models for the structural glass transition [39] it has never been possible to explore such low temperatures for comparable numbers of particles³. On the other hand such models [39] do not seem to be much plagued by finite size effects, although for certain models for structural glasses they have recently been found [68].

V. RELAXATION OF INDIVIDUAL SPINS IN THE LOW TEMPERATURE PHASE

In the previous section we have investigated the relaxation dynamics of the *whole* system and found that at low temperatures it shows a non-Debye behavior. In the present section we focus on the dynamics of the individual spins in order to obtain a better understanding for the occurrence of this non-exponentiality.

In recent years it has been recognized that the non-exponential relaxation in supercooled liquids is often related to the so-called “dynamical heterogeneities” [45,46]. This means that the details of the relaxation dynamics of the individual particles (relaxation time, amplitude of the α -relaxation, etc.) is different for each different particle. The reason for this difference is (most likely) the fact that each particle has a slightly different neighborhood which thus affects the dynamics of the particle. Note that these differences are present only on the time scale of the α -relaxation τ , since afterward the particle has changed its neighborhood and hence its characteristic dynamics. If the dynamics is averaged over a time much larger than τ , all the particles behave the same. For spin glasses this is different, since the disorder is quenched. Hence the nature of the dynamics of the individual spins is an intrinsic property of each spin, since each spin is connected to the other ones by a set of different coupling constants. For a spin glass with short range interactions it is therefore not surprising that each individual spin has a different relaxation dynamics, and this is indeed what has been found in simulations [65]. For spins systems with long range interactions the presence of such dynamical heterogeneities is, however, not that clear, since each spin interacts with many different ones and hence one might argue that on average the different spins show the same relaxation dynamics. The goal of this section is to investigate this point in more detail.

In order to characterize the dynamics of the individual spins we have calculated the autocorrelation functions $C_i(t)$ for spin number i :

³An exception are simulations of strong glass formers. E.g. in Ref. [64] it was shown that the system could be equilibrated even at temperatures as low as $0.8T_D$. However, one was still way above the Kauzmann temperature.

$$C_i(t) = \frac{1}{p-1} \langle \vec{S}_i(t') \cdot \vec{S}_i(t' + t) \rangle. \quad (39)$$

Note that, in contrast to the case of structural glasses, it is here possible to average the right hand side over different time origins t' , without loosing the information on the identity of the spin. Due to the single spin nature of the correlation function $C_i(t)$ it is necessary to make this average over a sufficiently long time in order to obtain a reasonable statistics. We found that an average over 1000 α -relaxation times is needed, and therefore the following results have been obtained only for relatively small system sizes and 10 different samples for every temperature investigated.

In Fig. 14 we show the time dependence of $C_i(t)$ for all the spins $i = 1, \dots, N$ for three different system sizes N . The temperature is T_D , i.e. the dynamical critical temperature at which the *average* relaxation dynamics, as measured by $C(t)$, is already strongly non-exponential. From the figure we see that the relaxation dynamics for the different spins depends strongly on these spins in that, e.g., they relax to zero on time scales that span more than an order of magnitude. At a time where the correlation functions have reached 0.5 of their initial value, the width of the range is even higher and increases rapidly with increasing system size. Furthermore we see from the figures that the curves for the individual spins seem to occur in clusters, i.e. that they do not fill the interval between the slowest and the fastest relaxation in a homogeneous way. Below we will discuss the reason for this clustering in more detail.

In Fig. 15 we show the single spin autocorrelation function at a lower temperature. Comparing these curves with the ones in Figs. 14a and 14b we see that a decrease of T has made the distribution of the relaxation dynamics even wider. Also the presence of the clustering of the curves is now much more pronounced. From Fig. 15 one also recognizes that the shape of the individual curves is not uniform at all since the ones which decay slowly tend to be, in the α -regime, much steeper than the ones that decay more rapidly. A more careful analysis shows that these slow spins show more or less an exponential relaxation whereas, as can already be seen from the figure, the fast ones show a strong deviation from a Debye law. Thus we conclude that the non-Debye behavior of $C(t)$ found at low T , see Fig. 12, is not due to a superposition of Debye laws with different relaxation times, but the sum of various different processes, some of which are Debye-like, some of which are not.

In order to understand the microscopic reason for the presence of these dynamical heterogeneities a bit better we have investigated to what extent the relaxation dynamics of an individual spin correlates with other quantities. For this it is necessary to characterize this dynamics in some way. As discussed above, the shape of the curves is not at all uniform, which makes such a characterization rather difficult. Therefore we decided to neglect all the variations of the shape completely and to characterize each curve just by the time it takes the spin to decay to a given value. Therefore we defined two different relaxation times, $\tau_i^{(0.4)}$ and $\tau_i^{(0.7)}$, via

$$C_i(t = \tau_i^{(0.4)}) = 0.4 \text{ and } C_i(t = \tau_i^{(0.7)}) = 0.7. \quad (40)$$

In Fig. 16 we show a scatter plot between $\langle e_i \rangle$, the average energy of spin i , and the relaxation time, for both definitions of τ_i . We see that there is indeed a significant correlation between the energy and the relaxation time in that spins with high energy relax faster than

the ones with low energy. This result is very reasonable since a spin that has a low energy will be reluctant to change its value and therefore to go (with high probability) to a state with a higher energy. From the figure we also recognize that the correlation is present for both definitions of τ_i , from which we conclude that the details of this definition are not crucial.

In order to investigate this point a bit closer we show in Fig. 17a a scatter plot of the relaxation time $\tau_i^{(0.7)}$ versus $\tau_i^{(0.4)}$ for the two temperatures. We see that although the correlation is not perfect, it is still very significant and therefore we conclude that the salient features of the correlation between the relaxation time and the mean energy shown in Fig. 16 will be observed even if a more careful characterization of the relaxation dynamics is made.

Of further interest is the question how the relaxation time of a given spin at a given temperature is related to the relaxation time of the same spin at a different temperature. This dependence is related to the question of “chaos in temperature”, i.e. how the properties of a system change if temperature is changed. For mean field type system it is expected that these dependencies are rather weak [66,67]. In agreement with this expectation we find that indeed the relaxation times τ_i for $T = 0.9$ are strongly correlated with those at $T = 1.142$, see Fig. 17b, irrespective of the definition of τ_i . Thus we see that this property seems not to be strongly affected by finite size effects. In passing we also mention that the mean energies $\langle e_i(T) \rangle$ between the two temperatures are even much stronger correlated than the relaxation times [51].

Before we end we come back to the observation discussed above that some of the single spin autocorrelation functions occur in clusters (see Fig. 15). One potential reason that the relaxation dynamics of two spins is similar is that they are coupled together strongly, i.e. that their interaction constant J_{ij} is large. In order to test this idea we identified for each realization of the disorder those spins that formed at $T = 0.9$ the cluster that relaxed slowest. (This identification was done visually by means of plots like the one shown in Fig. 15b). Say that this cluster involved k curves. We then determined the $k(k - 1)/2$ interaction constants between these k spins. The values of these constants are shown in Fig. 18 for ten different realizations of the disorder (filled circles). Also included in the figure is the Gaussian distribution of the coupling constants given by Eq. (2). From this figure we see that most of the points corresponding to the couplings J_{ij} are to the right of the mean of the distribution (vertical dashed line). Hence we conclude that the spins that form the slow cluster of relaxation curves are coupled together stronger than two arbitrary spins and therefore form a “dynamic entity”. We note, however, that the fact that two spins are strongly coupled does not necessarily make them slow [51] which shows that such a strong coupling is only a necessary but not a sufficient condition for a slow dynamics.

It is clear that the observations presented in this section are only modest first steps addressing the dynamics of the individual spins in the low temperature phase. It certainly would be interesting and useful to understand better how the distribution of the relaxation times of the spins depends on the system size and on temperature in order to obtain a better comprehension how the mean relaxation dynamics of the system is related to the one of the single spins. However, due to the high computational demand for this kind of investigations such studies have to be left to the future.

VI. CONCLUSIONS

In this paper, we have presented the first detailed Monte Carlo investigation of the 10 state mean field Potts glass model, for finite systems with sizes in the range from $N = 160$ to $N = 2560$ spins. In the thermodynamic limit, it is known that this model exhibits both a dynamical transition at T_D where the system stops to be ergodic, and a static transition at $T_0 < T_D$ where a glass order parameter q appears discontinuously (Fig. 5a). The static spin glass susceptibility χ_{SG} remains finite both at T_0 and T_D . It would diverge only at a still lower “spinodal” temperature $T_s < T_0$, if one were able to follow the disordered branch of the free energy at temperatures less than T_0 . A further relevant temperature is the “Kauzmann” temperature T_K , Fig. 1c, defined from the condition that the entropy of the high temperature phase vanishes. The spin autocorrelation function $C(t)$ decays with time t at $T \gtrsim T_D$ in a two-step process, and the lifetime τ of the “plateau” diverges as $\tau \propto (T - T_D)^{-\Delta}$, in the thermodynamic limit $N \rightarrow \infty$ (Fig. 5a). This behavior entails all qualitative features that one expects to be present at the structural glass transition (note that the equation of motion for $C(t)$ indeed is described by the popular idealized mode-coupling theory proposed for the structural glass transition!).

The questions asked in the present paper hence are as follows: can we verify these predictions from Monte Carlo simulations? How are the various transitions modified (i.e., rounded off) by the finite size of the considered model systems? Answers to these questions are not only of interest for a better understanding of the statistical mechanics of the present model system, they may also be useful to help with the interpretation of simulations of models for the structural glass transition. First of all, in the latter case the very existence of the various temperatures T_D , T_0 , T_s , T_K is still open to doubt. Secondly, even if one believes these temperatures should exist, their location for a particular model is still uncertain, unlike the present case where we have so much guidance from the exact solution. Of course, it is clear that a mean-field model is a rather special limit, and the sharpness of the dynamical transition at T_D probably is replaced by a smooth crossover from rather fast relaxation to very slow relaxation, as soon as one allows the interactions to become short ranged. In this sense, the finite mean-field Potts glass (where the singularity at T_D is rounded by the finite size of the system) may be qualitatively similar to the finite range model (although one should not push this analogy too far).

Gratifyingly, we have established that the Monte Carlo results are qualitatively compatible with the theoretical predictions, although the finite size effects found were unexpectedly strong (i.e. they occur over a very wide temperature range as well) and they are not understood in detail, and hence we have found it too difficult to extract the various temperatures mentioned above directly from the simulation itself. E. g., for the sizes available, the method of looking for intersection points of the fourth order cumulant or the Guerra parameter do not allow for a reliable estimation of T_0 (Fig. 4). Similarly, one could estimate the temperatures T_s (Fig. 2), T_K (Fig. 1b) and T_D (Fig. 8) from a naive analysis of the data only very roughly. However, if one uses the theoretical knowledge on T_D , one can estimate both the exponent Δ mentioned above and the exponent z^* for the size dependence of the time τ at T_D ($\tau \propto N^{z^*}$) from a dynamical finite size scaling analysis (Fig. 9). We also found evidence that the predicted power law decay of the spin autocorrelation function $C(t) - q_{EA} \propto t^{-a}$ occurs for $T \approx T_D$ (Fig. 10), but we could not confirm the expected time-temperature

superposition principle (Fig. 11). We also analysed the modified disconnected cumulants proposed in reference [71], which should give a better estimation of the spin glass transition temperature in systems exhibiting one step replica symmetry breaking patterns, but with the system sizes at our disposal they do not seem to work better than the corresponding connected parameters [51].

Also some steps were taken to analyze the dynamics for $T \leq T_D$, by investigating the relaxation function $C_i(t)$ of individual spins and corresponding relaxation times (Figs. 14-17). We find that the reason for the observed non-exponential relaxation of the *mean* relaxation function $C(t)$ is related to the presence of a very strong dynamical heterogeneity. Furthermore we found that certain spins form dynamical clusters, the reason for which are likely their strong bonds between them. However, this mechanism seems not to be the only one and hence this point has to be investigated in the future in more detail.

Thus, although many exact results are known for this model, and - unlike in models of the structural glass transition - we can equilibrate the system also at temperatures significantly below T_D for a range of sizes ($N \leq 640$), we still are not able to answer many questions. Nevertheless, we think that the present model is a prototype model for glass transitions, and if better simulation algorithms become available, further studies of the present model should be very rewarding.

Acknowledgements: One of us (C.B) was partially supported by the Deutsche Forschungsgemeinschaft, Sonderforschungsbereich 262/D1. We thank F. Ritort for information on the energy vs. temperature curve (Fig. 1a). We are grateful to the John von Neumann Institute for Computing (NIC Jülich) for a generous grant of computer time at the CRAY T3E.

REFERENCES

- [1] Monasson R 1995 *Phys. Rev. Lett.* **75** 2847
- [2] Bouchaud J-P, Cugliandolo L, Kurchan J, and Mézard M 1998 in *Spin Glasses and Random Fields*, ed. A P Young, World Scientific (Singapore)
- [3] Franz S and Parisi G 1998 *Physica A* **261** 317
- [4] Mézard M and Parisi G 1999 *Phys. Rev. Lett.* **82** 747
- [5] Kirkpatrick T R and Wolynes P G 1987 *Phys. Rev. B* **36** 8552; Kirkpatrick T R and Thirumalai D 1988 *Phys. Rev. B* **37** 5342; Thirumalai D and Kirkpatrick T R 1988 *Phys. Rev. B* **38** 4881
- [6] Götze W 1990 in *Liquids, Freezing and the Glass Transition*, Hansen J P, Levesque D and Zinn-Justin J, eds. (Amsterdam, North Holland) p. 287; *J. Phys.: Condens. Matter* **11** A1
- [7] Elderfield D and Sherrington D 1983 *J. Phys. C: Solid State Phys.* **16** L491, L971, L1169
- [8] Erzan A and Lage E J S 1983 *J. Phys. C: Solid State Phys.* **16** L55
- [9] Gross D J, Kanter I and Sompolinsky H 1985 *Phys. Rev. Lett.* **55** 304
- [10] Carmesin H O and Binder K 1988 *J. Phys. A: Math. Gen.* **21** 4053
- [11] Cwiliich G and Kirkpatrick T R 1989 *J. Phys. A: Math. Gen.* **22** 4971; Cwiliich G 1990 *J. Phys. A: Math. Gen.* **23** 5029
- [12] Scheucher M, Reger J D, Binder K and Young A P 1990 *Phys. Rev. B* **42** 6881; *Europhys. Lett.* **14**, 119; Scheucher M and Reger J D 1993 *Z. Phys. B* **91** 383
- [13] De Santis E, Parisi G and Ritort F 1995 *J. Phys. A: Math. Gen.* **28** 3025
- [14] Schreider G and Reger J D 1995 *J. Phys. A: Math. Gen.* **28** 317
- [15] Reuhl M, Nielaba P and Binder K 1999 *Eur. Phys. J. B* **2** 225
- [16] Dillmann O, Janke W and Binder K 1998 *J. Stat. Phys.* **92** 57
- [17] Lobe B, Janke W and Binder K 1999 *Eur. Phys. J. B* **7** 289
- [18] Marinari E, Mossa S and Parisi G 1999 *Phys. Rev. B* **59**, 8401
- [19] Hukushima K and Kawamura H 2000 *Phys. Rev. E* **62**, 3362
- [20] Edwards S F and Anderson P W 1975 *J. Phys. F: Metal Physics* **5** 965
- [21] Sherrington D and Kirkpatrick S 1975 *Phys. Rev. Lett.* **35**, 1972
- [22] Binder K and Young A P 1986 *Rev. Mod. Phys.* **58** 801
- [23] Mézard M, Parisi G and Virasoro M A 1987 *Spin Glass Theory and Beyond* (Singapore, World Scientific)
- [24] Fischer K H and Hertz J A 1991 *Spin Glasses* (Singapore, World Scientific)
- [25] Stein D S 1992 *Spin Glasses and Biology* (Singapore, World Scientific)
- [26] Parisi G 1992 *Field Theory, Disorder and Simulations* (Singapore, World Scientific)
- [27] Young A P (ed.) 1998 *Spin Glasses and Random Fields* (Singapore, World Scientific)
- [28] Potts R B 1952 *Proc. Camb. Phil. Soc.* **48** 106
- [29] Wu F Y 1982 *Rev. Mod. Phys.* **54** 235; *ibid.* **55** 315
- [30] Zia R K P and Wallace D J 1975 *J. Phys. A: Math. Gen.* **8** 1495
- [31] Kauzmann W 1948 *Chem. Rev.* **43** 219
- [32] Gibbs J H and DiMarzio E A 1958 *J. Chem. Phys.* **28** 373
- [33] Jäckle J 1986 *Rep. Progr. Phys.* **49** 171
- [34] Parisi G 1987 in *Complex Behavior of Glassy Systems* Rubi M and Perez-Vicente, eds. (Berlin, Springer) p. 111
- [35] Binder K, Baschnagel J, Kob W and Paul W 1999 *Physics World* **12**, 54

- [36] Coluzzi B, Verrocchio P, Mézard M and Parisi G 1999 *J. Chem. Phys.* **111** 9039
- [37] Sciortino F, Kob W and Tartaglia P 1999 *Phys. Rev. Lett.* **83** 3214
- [38] Crisanti A and Ritort F 2000 *Europhys. Lett.* **51** 147
- [39] Kob W 1999 *J. Phys.: Condens. Matter* **11** R85
- [40] Mézard M 1999 *Physica A* **265** 359
- [41] Parisi G 2000 *Physica A* **280** 115
- [42] Höchli U T, Knorr K and Loidl A 1990 *Adv. Phys.* **39** 405
- [43] Binder K and Reger J D 1992 *Adv. Phys.* **41** 547
- [44] Binder K in Ref. [27] p. 99
- [45] Sillescu H 1999 *J. Noncryst. Solids* **243** 81
- [46] Ediger M D 2000 *Annu. Rev. Phys. Chem.* **51** 99
- [47] Guerra F 1996 *Int. J. Mod. Phys. B* **10** 1675 Marinari E et al. 1998 *Phys. Rev. Lett.* **81** 1698
- [48] Binder 1997 *Rep. Progr. Phys.* **60** 487; Landau D P and Binder K 2000 *A Guide to Monte Carlo simulations in statistical Physics* (Cambridge, Cambridge Univ. Press)
- [49] Hukushima K and Nemoto K 1996 *J. Phys. Soc. Jpn.* **64** 1604
- [50] Kob W, Brangian C, Stühn T and Yamamoto R 2000 in *Computer Simulation Studies in Condensed Matter Physics XIII* Landau D P, Lewis S P and Schüttler H B, eds, (Berlin, Springer) p. 134
- [51] Brangian C 2001 Dissertation (Johannes-Gutenberg-Universität Mainz, in preparation)
- [52] Binder 1981 *Z. Phys. B* **45** 61
- [53] Ritort F, *private communication*
- [54] Wolfgardt M, Baschnagel J, Paul W and Binder K 1996 *Phys. Rev. E* **54** 1535
- [55] Binder K 1992 in *Computational Methods in Field Theory*, Gausterer H and Lang C B, eds, (Berlin, Springer) p. 59
- [56] Vollmayr K, Reger J D, Scheucher M and Binder K 1993 *Z. Phys. B* **91** 113
- [57] Brangian C, Kob W, and Binder K 2001 *Europhys. Lett.* **53** 756
- [58] Suzuki M 1977 *Progr. Theor. Phys.* **58** 1142
- [59] Hohenberg P C and Halperin B I 1977 *Rev. Mod. Phys.* **49** 435
- [60] Bhatt R N and Young A P 1992 *Europhys. Lett.* **20** 59
- [61] Jayaprakash C, Chalupa J and Wortis M 1977 *Phys. Rev. B* **15** 1495
- [62] Mackenzie N D and Young A P 1983 *J. Phys. C* **16** 5321
- [63] Billoire A and Marinari E preprint cond-mat/0101177
- [64] Horbach J and Kob W 1999 *Phys. Rev. B* **60** 3169
- [65] Glotzer S C, Jan N and Poole P H 1998 *Phys. Rev. E* **57** 7350
- [66] Kondor I 1989 *J. Phys. A: Math. Gen.* **22** L163
- [67] Ritort F 1994 *Phys. Rev. B* **50** 6844
- [68] Kim K and Yamamoto R 2000 *Phys. Rev. E* **61** R41
- [69] Biroli G and Monasson R 2000 *Europhys. Lett.* **50** 155
- [70] Parisi G, Ritort F and Slanina F 1998 *J. Phys. A* **26** 247 ; 1998 *ibid.* **26** 3775
- [71] Picco M, Ritort F and Sales M 2001 *Eur. Phys. J. B* **19** 565

FIGURES

fig1a

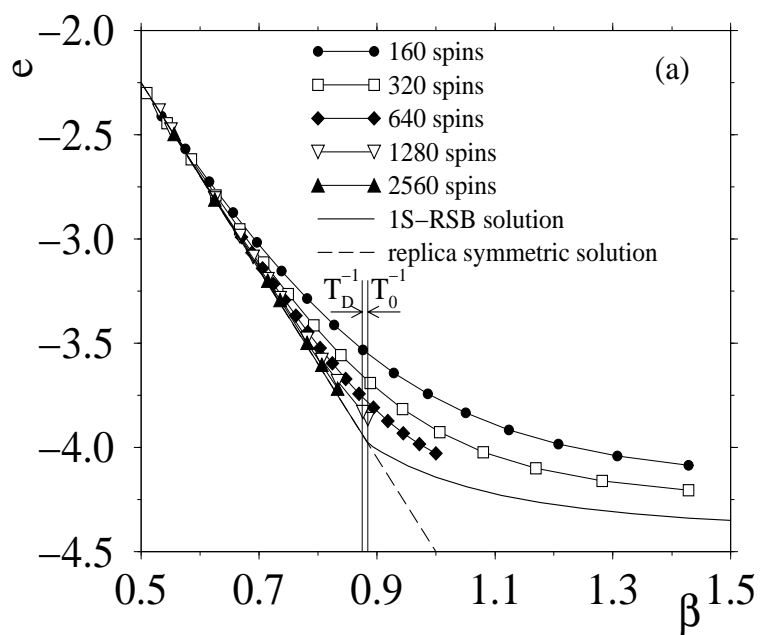
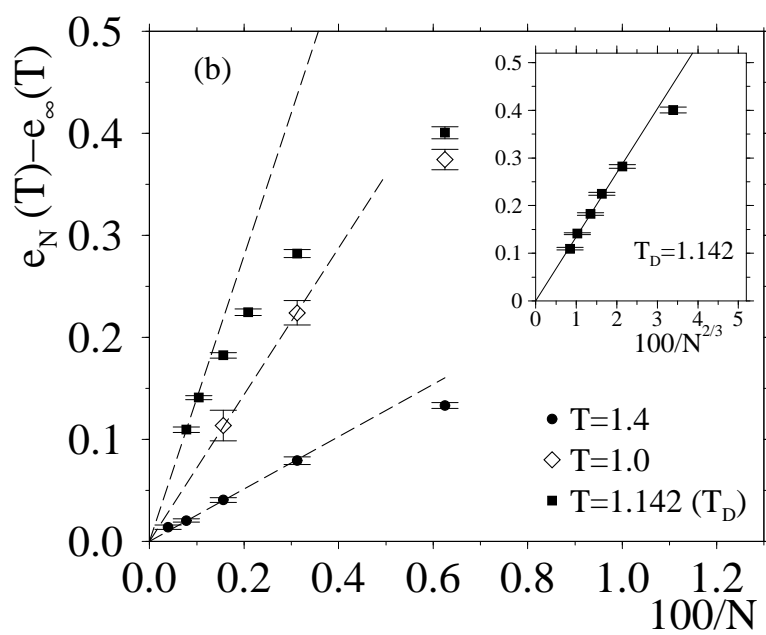


fig1b



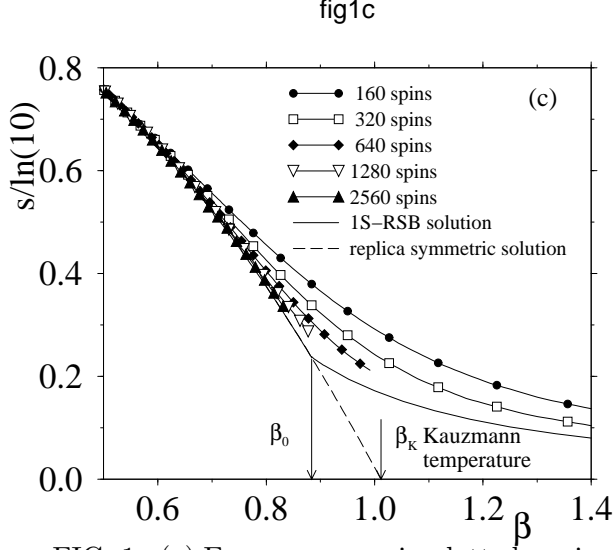


FIG. 1. (a) Energy e per spin plotted vs. inverse temperature $\beta = 1/T$ for different system sizes (curves with symbols). The bold solid curve shows the one step replica symmetry breaking solution of DeSantis *et al.* [13,53], the broken curve - which coincides with the former for $T \geq T_0$ - is the replica symmetric solution, Eq. (25). The thin vertical lines indicated the inverse temperatures β_D (left) and β_0 (right) of the dynamical transition and the static transition, respectively. (b) Analysis of the size dependence of the energy difference $e_N(T) - e_\infty(T)$, using the one-step replica symmetric solution of DeSantis *et al.* [13] to calculate $e_\infty(T)$. Inset shows the data of $T = T_D = 1.142$ plotted vs. $N^{-2/3}$ instead of N^{-1} . (c) Entropy s per spin, normalized by its high temperature value, plotted vs. inverse temperature for different system sizes (curves with symbols). The bold dashed and the bold solid curve is the replica symmetric solution and the one-step replica symmetry breaking solution, respectively. Vertical arrows indicate the static inverse transition temperature β_0 and the inverse of the “Kauzmann temperature” β_K , where the entropy of the replica symmetric solution vanishes.

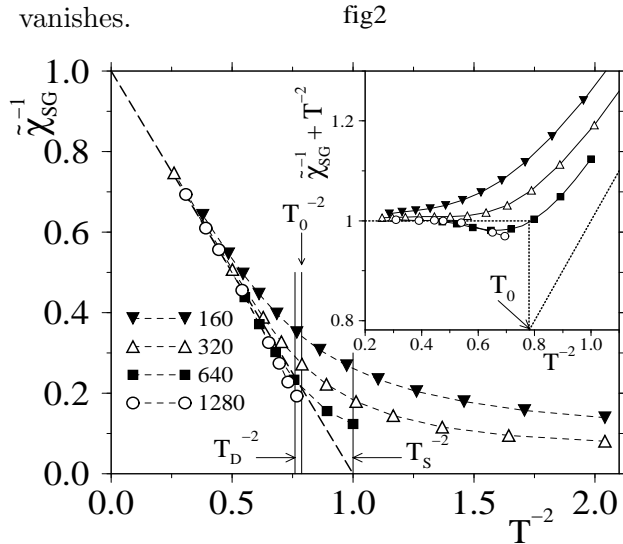


FIG. 2. Inverse of the reduced spin glass susceptibility $\tilde{\chi}_{SG}$ versus the square of inverse temperature for different system sizes (curves with symbols). The solid line shows the result of the replica-symmetric theory, Eq. (26). Inset: Plot of $\tilde{\chi}_{SG}^{-1} + (T_s/T)^2$ to illustrate the nonmonotonic convergence towards Eq. (26). See main text for more details.

fig3a

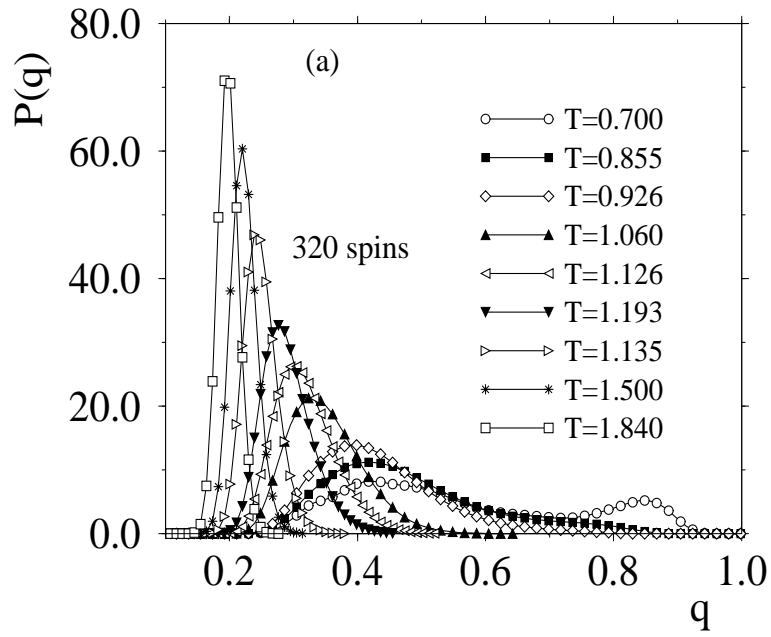


fig3b

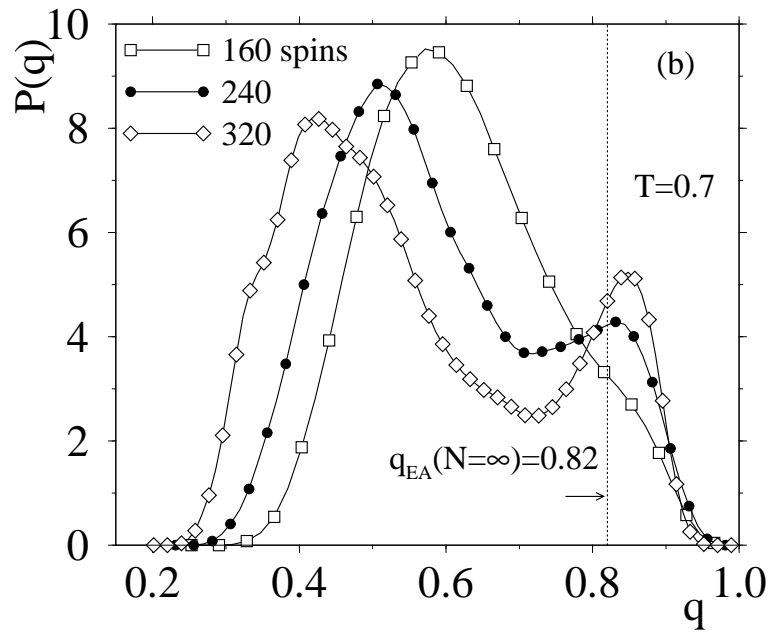


fig3c

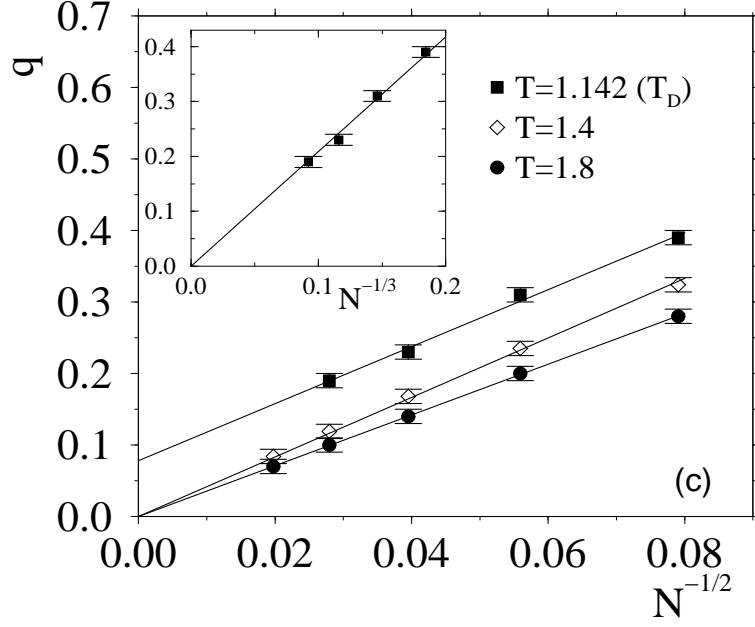


FIG. 3. (a) Order parameter distribution $P(q)$ versus q for $N = 320$ and various temperatures. (b) Order parameter distribution $P(q)$ versus q for $T = 0.7$ and the three system sizes $N = 160, 240$ and 320 . The asymptotic value of the order parameter (from Ref. [53]) is included by a vertical line. (c) Value of the first moment $\int qP(q) dq$ of the order parameter distribution vs. $N^{-1/2}$. The inset shows that close to the transition temperature $T_0 \approx T_D$ this moment scales like $N^{-1/3}$.

fig4a

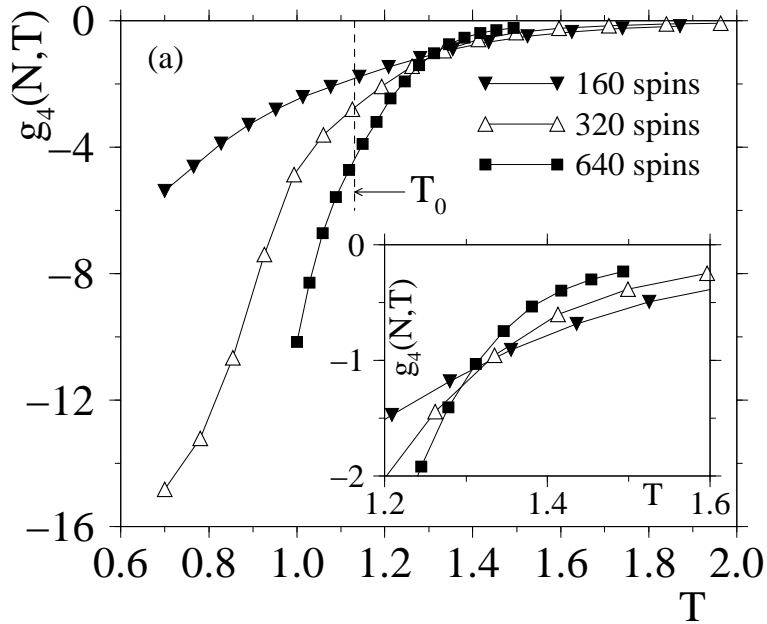


fig4b

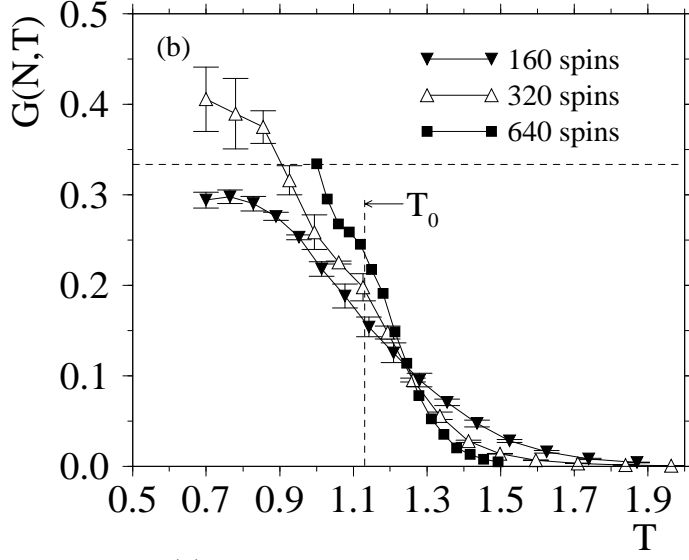
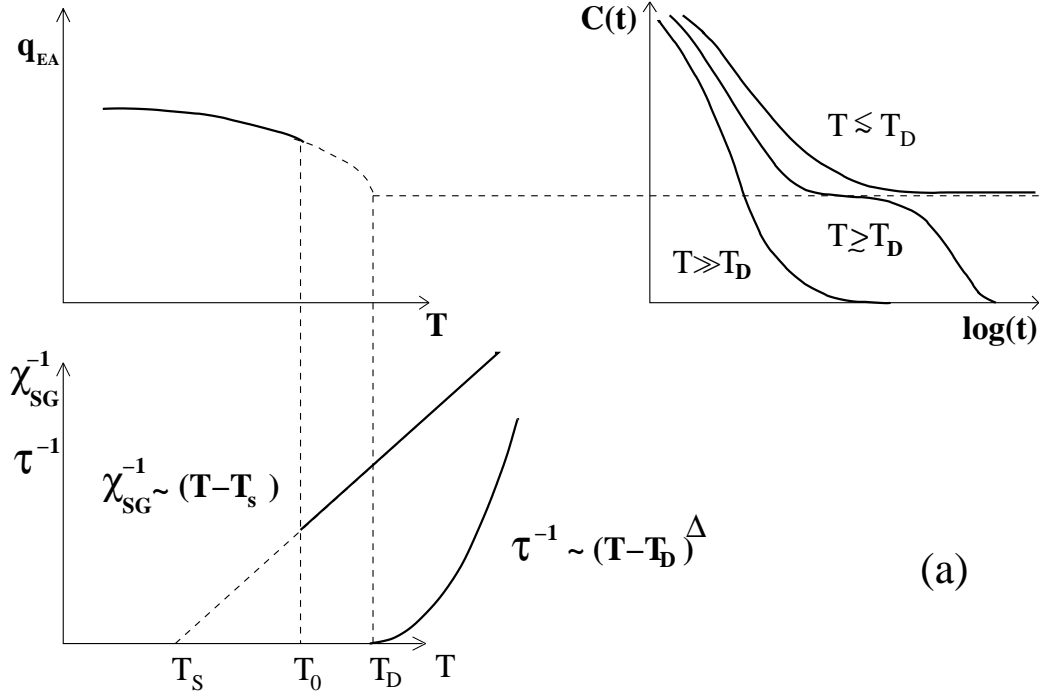


FIG. 4. (a) Fourth order cumulant g_4 plotted versus temperature, for three values of N , $N = 160, 320$ and 640 . The vertical straight line highlights the predicted static transition temperature T_0 . (b) Same as (a) but for the Guerra parameter. The horizontal dashed line is the theoretical expectation for $T < T_0$.



(a)

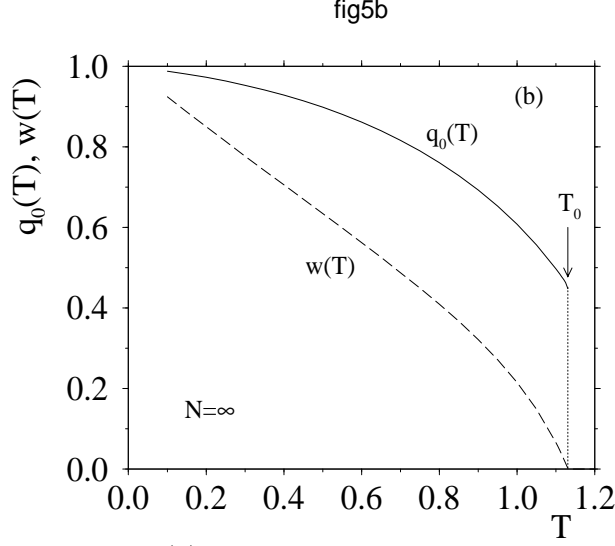


FIG. 5. (a) Qualitative sketch of the mean-field predictions for the p -state Potts glass model with $p > 4$. The spin glass order parameter, q_{EA} , is nonzero only for $T < T_0$ and jumps to zero discontinuously at $T = T_0$. The spin glass susceptibility χ_{SG} follows a Curie-Weiss-type relation with an apparent divergence at $T_s < T_0$, see Eq. (21). The relaxation time τ diverges already at the dynamical transition temperature T_D . This divergence is due to the occurrence of a long lived plateau of height q_{EA} in the time-dependent spin autocorrelation function $C(t)$. From Brangian *et al.* [57]. (b) Temperature dependence of q_0 and $w(T)$ (see Eq. (22)) for $p = 10$, as obtained from the one-step replica symmetric solution of DeSantis *et al.* [13].

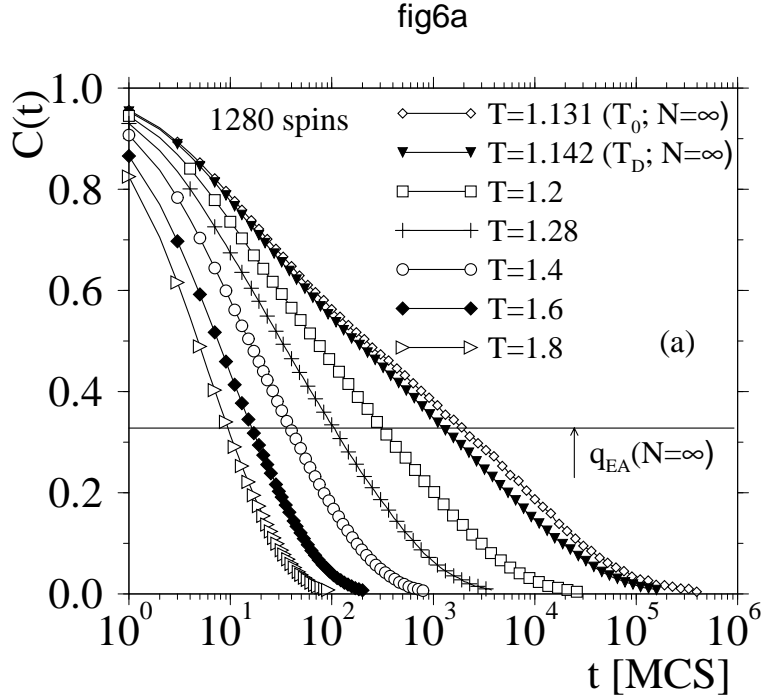


fig6b

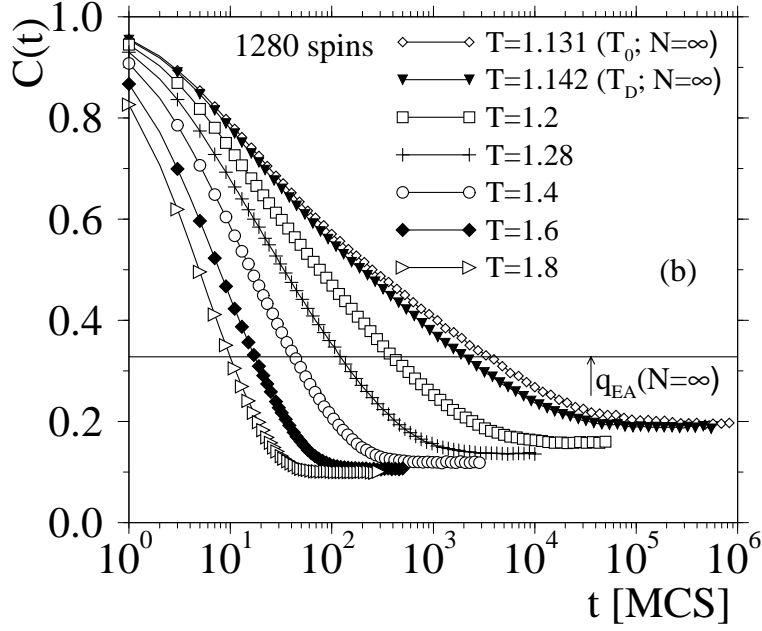
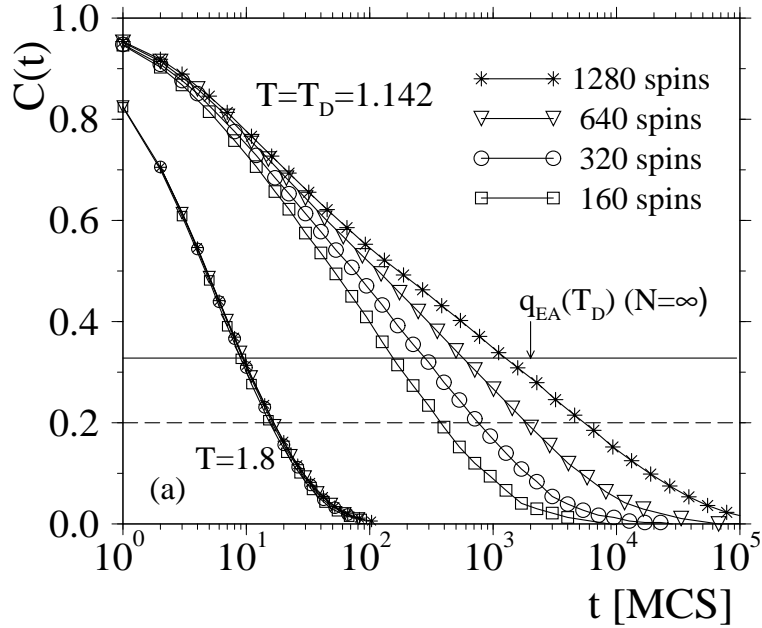


FIG. 6. (a) Time dependence of the correlation function $C(t)$, Eq. (13), for $N = 1280$ and various temperatures. Also included is data for the predicted values of the static, T_0 , and dynamic, T_D , transition temperature. The horizontal straight line shows the theoretical prediction from Ref. [13] for the Edwards-Anderson order parameter at T_D , $q_{EA} = \lim_{t \rightarrow \infty} C(t)$, cf. Eq. (32). (b) Same as (a) but for the rotationally invariant correlation function $C_{RI}(t)$ defined in Eq. (14).

fig7a



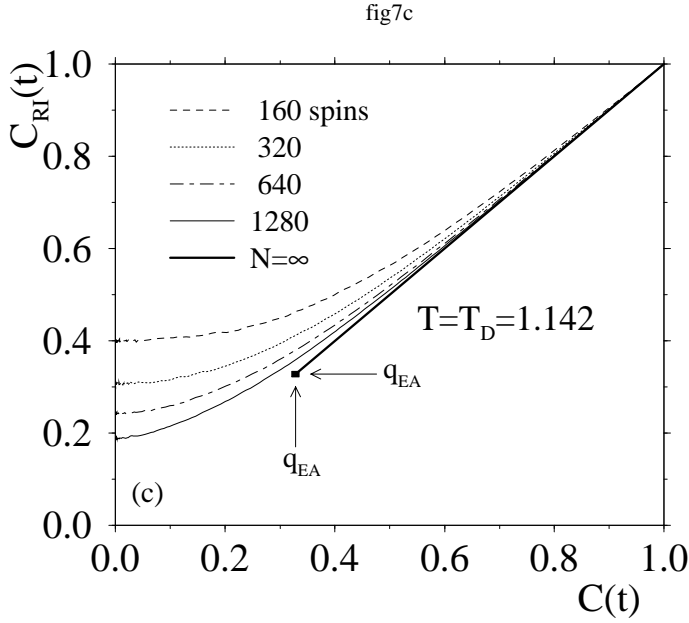
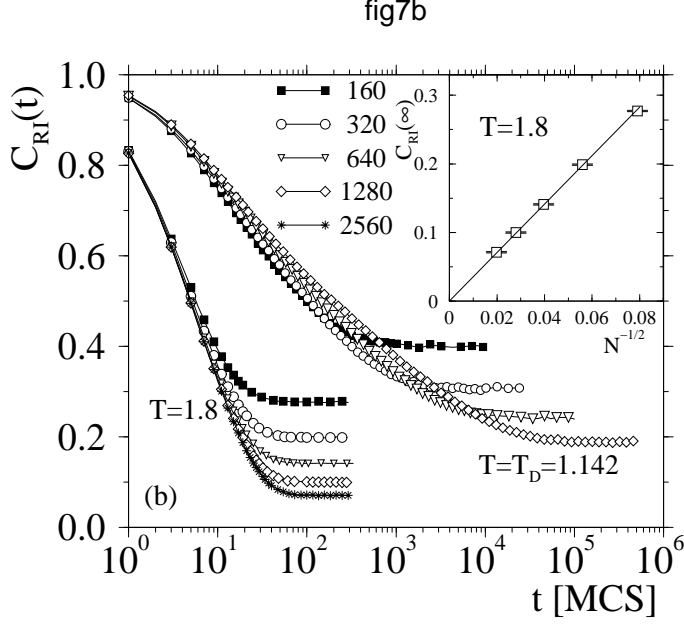


FIG. 7. (a) Time dependence of the correlation function $C(t)$ for $T = 1.8$ and for $T = T_D = 1.142$ for several values of N . The solid line is the theoretical value of the Edwards-Anderson order parameter $q_{EA}(T_D)$ for $N \rightarrow \infty$ [13]. The dashed line shows the value we use to define the relaxation time τ . From Brangian *et al.* [57]. (b) Time dependence of the rotationally invariant correlation function $C_{RI}(t)$ for $T = 1.8$ and for $T = T_D = 1.142$ for several values of N . The inset shows the limiting value $C_{RI}(t \rightarrow \infty)$ as a function of $N^{-1/2}$ for $T = 1.8$. (c) Parametric plot of $C_{RI}(t)$ vs. $C(t)$ at $T = T_D$ for different values of N . The square indicates the plateau value obtained for $N \rightarrow \infty$. The bold straight line describes the relation $C_{RI}(t) = C(t)$, believed to hold for $N \rightarrow \infty$.

fig8

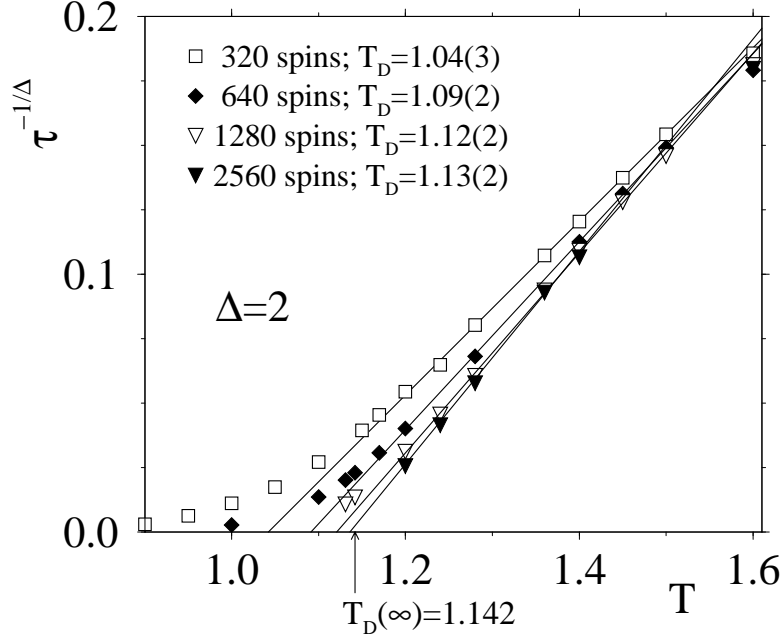


FIG. 8. Temperature dependence of $\tau^{-1/\Delta}$ for different system sizes, using $\Delta = 2.0$ as a trial value. The bold straight lines are fits on a proper subset of point. The resulting extrapolated values for $T_D(N)$ are quoted in the figure.

fig9

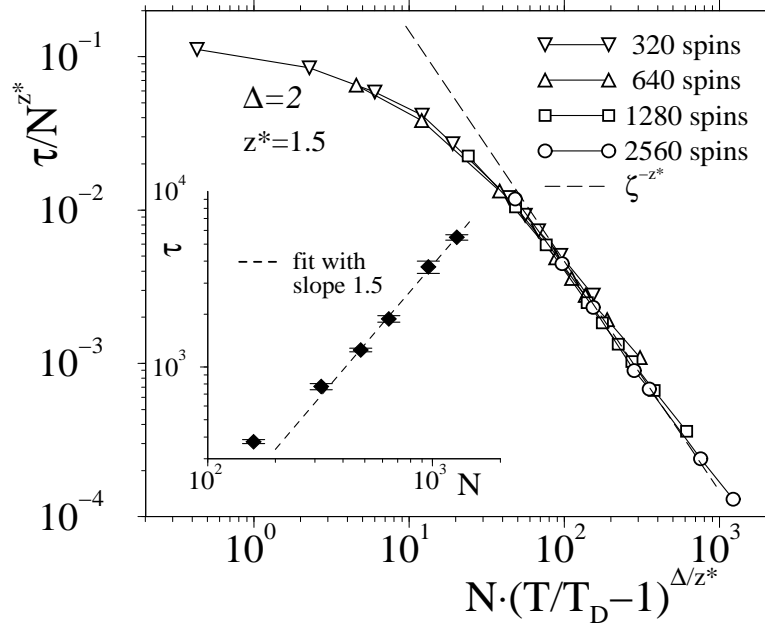


FIG. 9. Log-log plot of the scaled relaxation time τ/N^{z^*} vs the scaled distance $N(T/T_D - 1)^{\Delta/z^*}$ from the dynamical transition temperature T_D , choosing $z^* = 1.5$ and $\Delta/z^* = 1.3$. The inset is a log-log plot of $\tau(T = T_D)$ vs N .

fig10

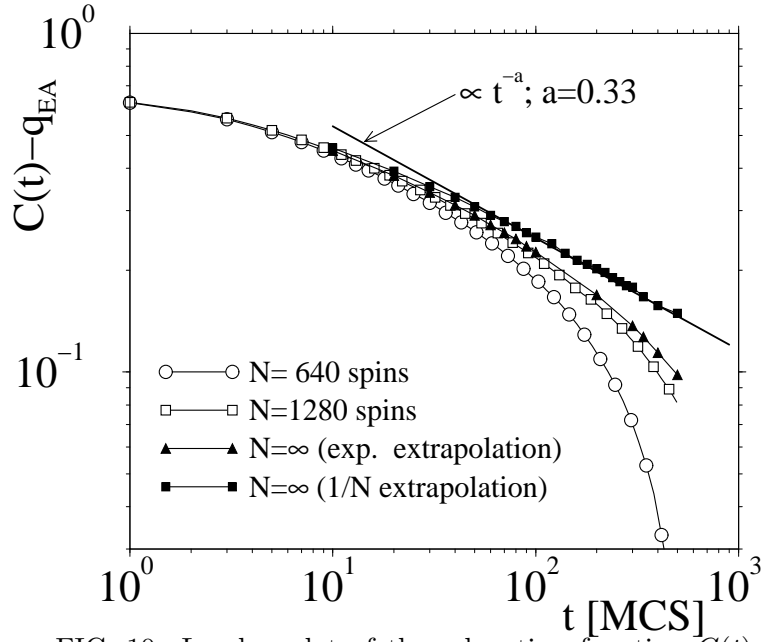


FIG. 10. Log-log plot of the relaxation function $C(t) - q_{EA}$ versus time for $T = T_D$, using the theoretical value of q_{EA} , Eq. (32). The curves with the open symbols are the data from the simulation for two system sizes. The two curves with the filled symbols are the extrapolation of the simulation data to the case $N = \infty$ (see main text for details). The bold solid line is a fit with a power law.

fig11

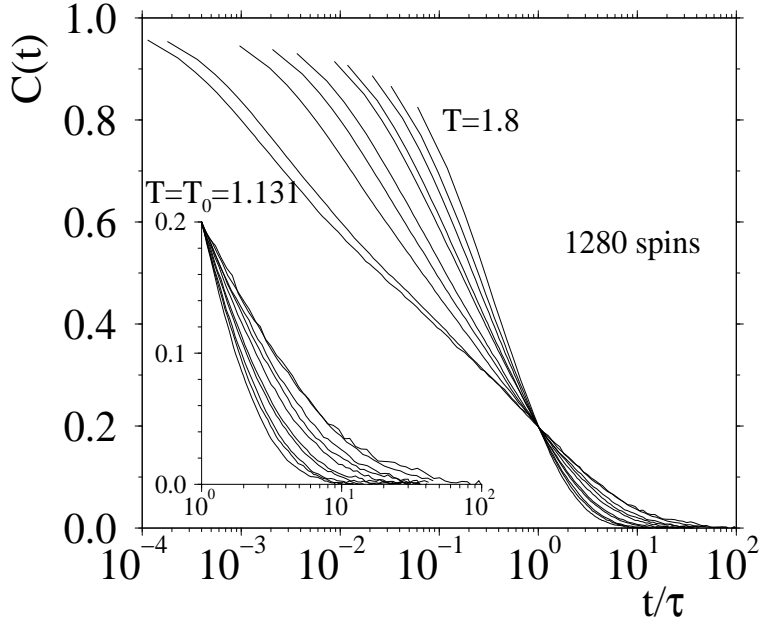


FIG. 11. Plot of $C(t)$ vs. t/τ (where τ is defined via $C(t = \tau) = 0.2$, cf. Eq. (33)), for $N = 1280$. Temperatures from right to left: $T = 1.8, 1.6, 1.5, 1.4, 1.360, 1.280, 1.240, 1.2, 1.142$, and 1.131 . The inset shows a magnification of the part of the curves for $t/\tau > 1$.

fig12

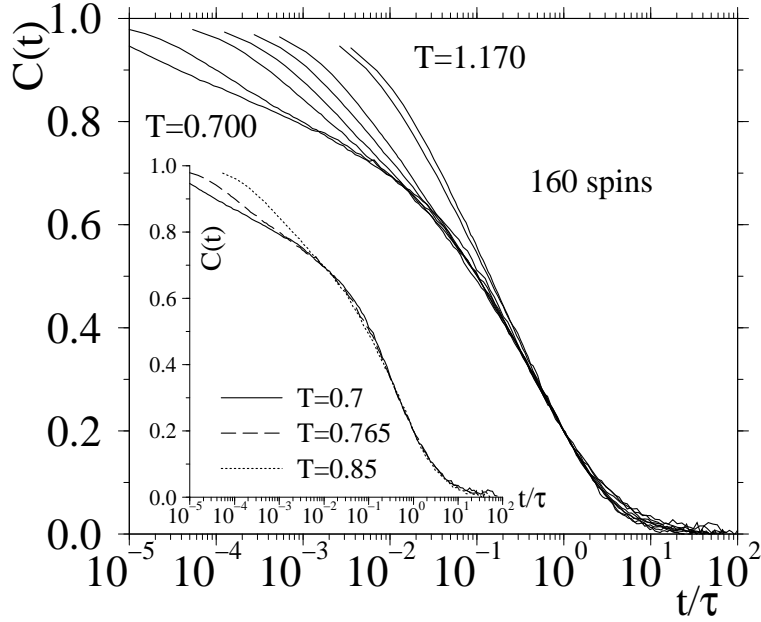


FIG. 12. Plot of $C(t)$ vs. t/τ for $N = 160$. The temperatures are $T = 0.7, 0.765, 0.85, 0.9, 0.95, 1.0, 1.142, \text{ and } 1.17$ (left to right). The inset shows the same data, but including only the three lowest temperatures.

fig13

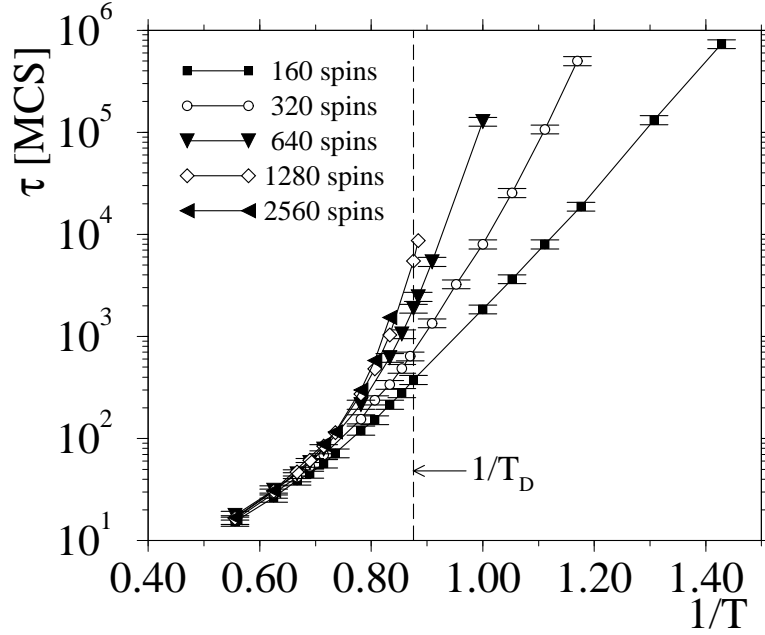


FIG. 13. Relaxation time τ plotted vs. inverse temperature for different system sizes. The broken vertical line indicates the location of the dynamical transition. Note the choice of a logarithmic scale for the ordinate. Error bars of τ are mostly due to the sample-to-sample fluctuation.

fig14a

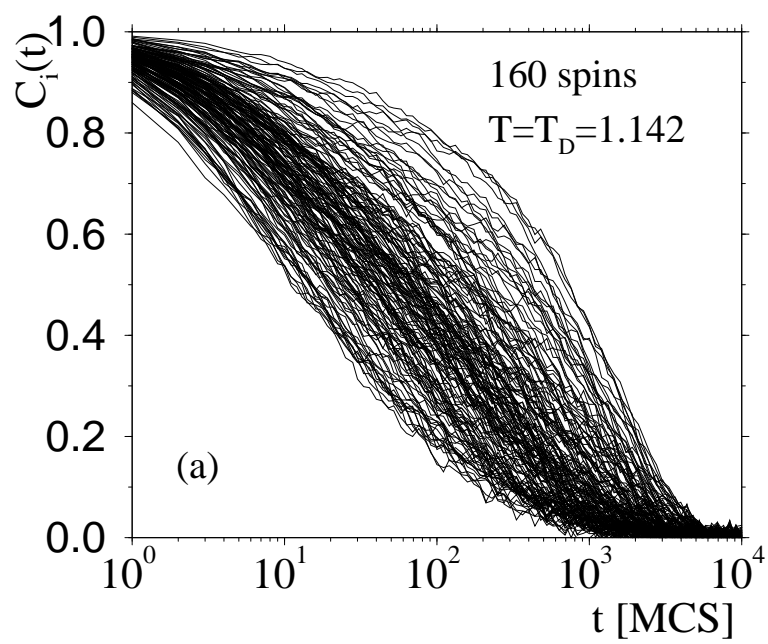


fig14b

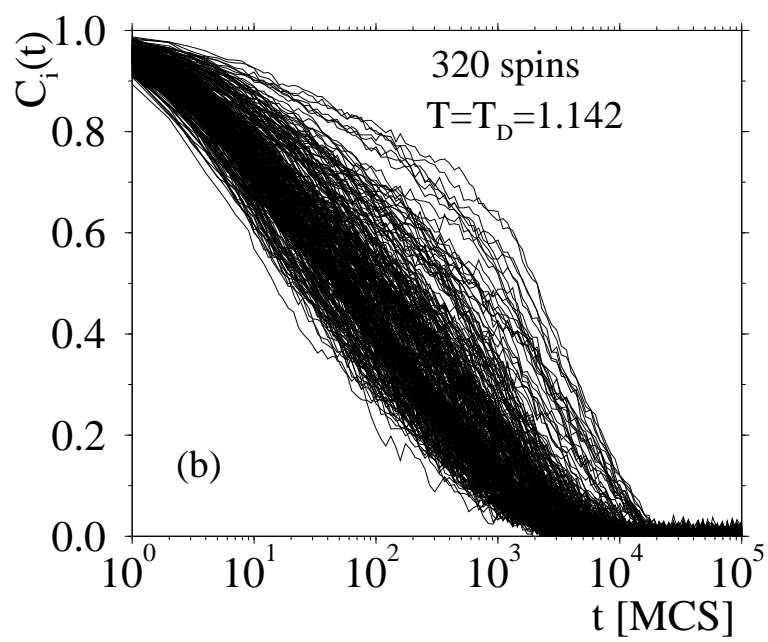


fig14c

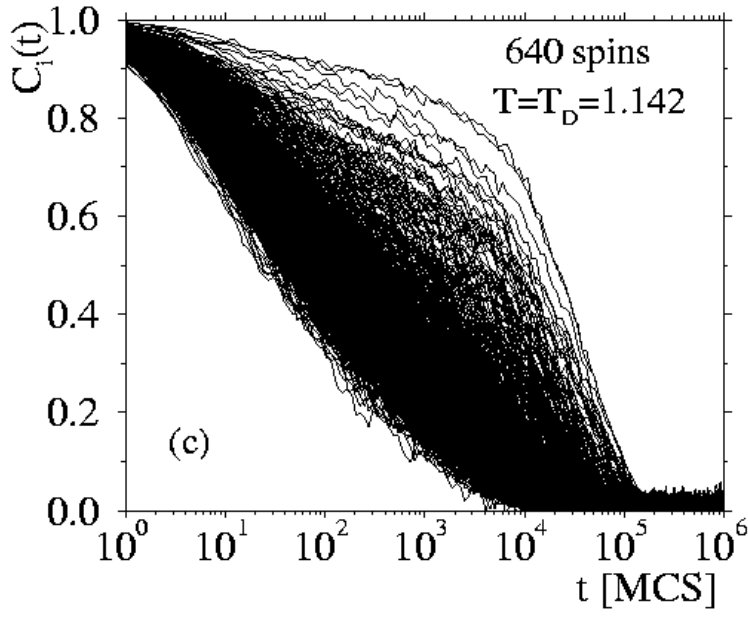


FIG. 14. Time dependence of the single spin autocorrelation function $C_i(t)$ at $T = T_D$ for $N = 160$ (a), $N = 320$ (b), and $N = 640$ (c). Each of the curves corresponds to a different spin.

fig15a

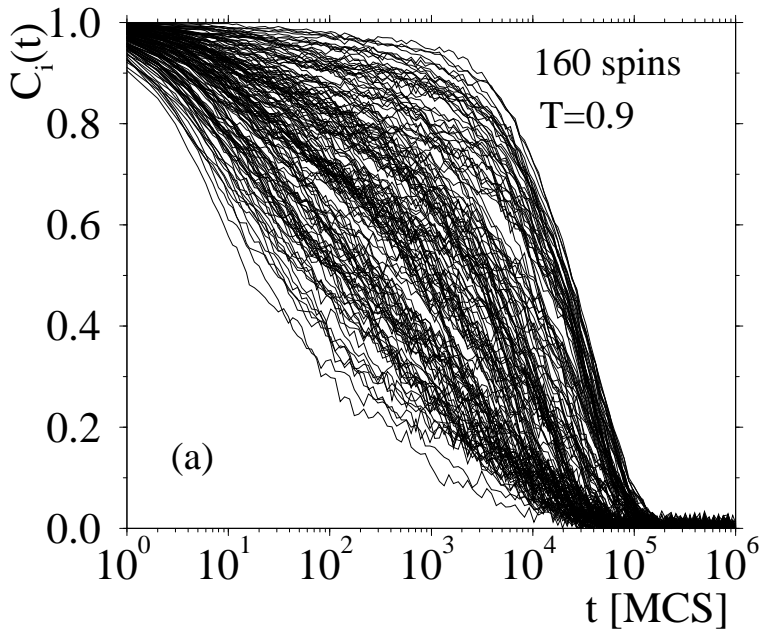


fig15b

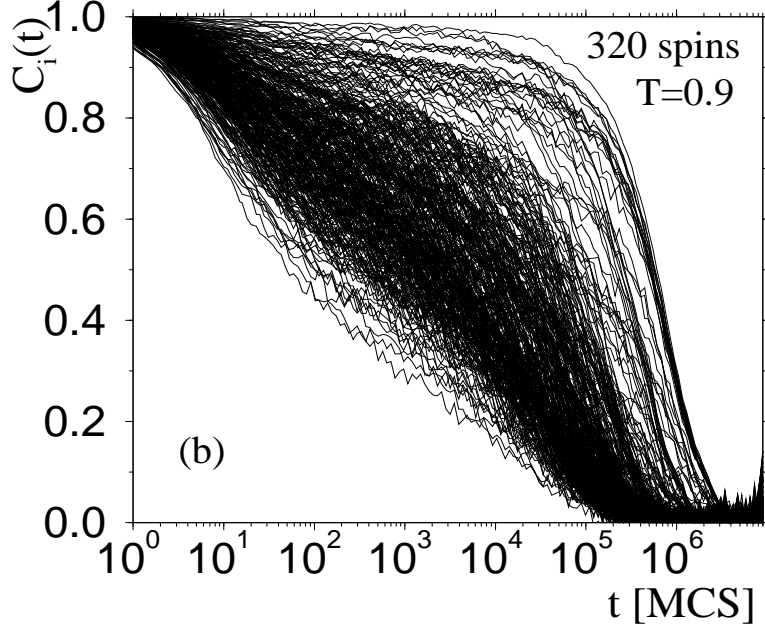


FIG. 15. Time dependence of the single spin autocorrelation function $C_i(t)$ at $T = 0.9$ for $N = 160$ (a) and for $N = 320$ (b). Each of the curves corresponds to a different spin.

fig16

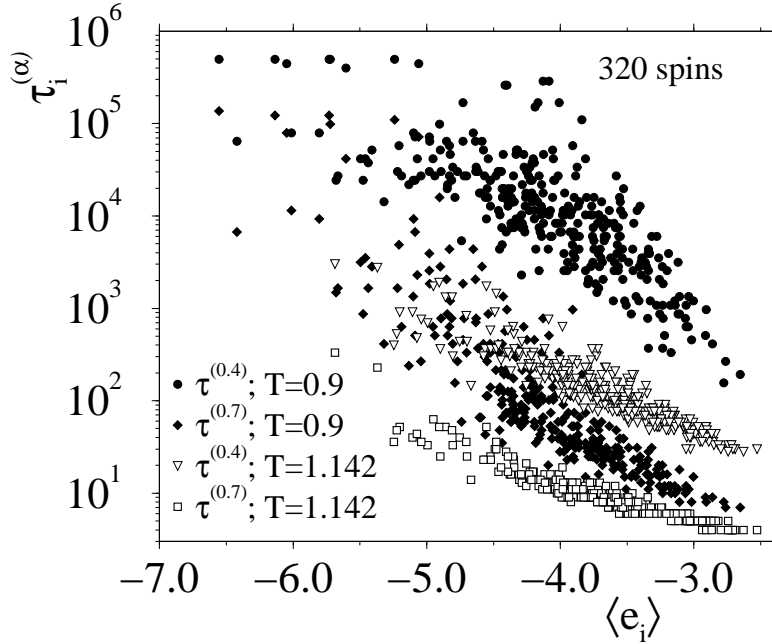


FIG. 16. Scatter plot of τ_i , the mean relaxation time of spin i as defined in Eq. (40), versus the mean energy $\langle e_i \rangle$. The open and closed symbols correspond to $T = 1.142$ and $T = 0.9$, respectively. The points are for a typical sample of 320 spins.

fig17a

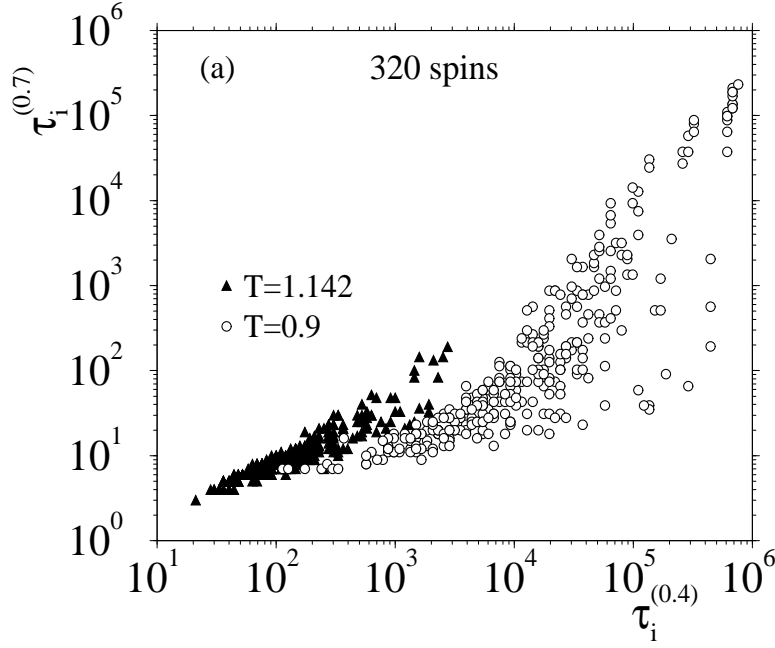


fig17b

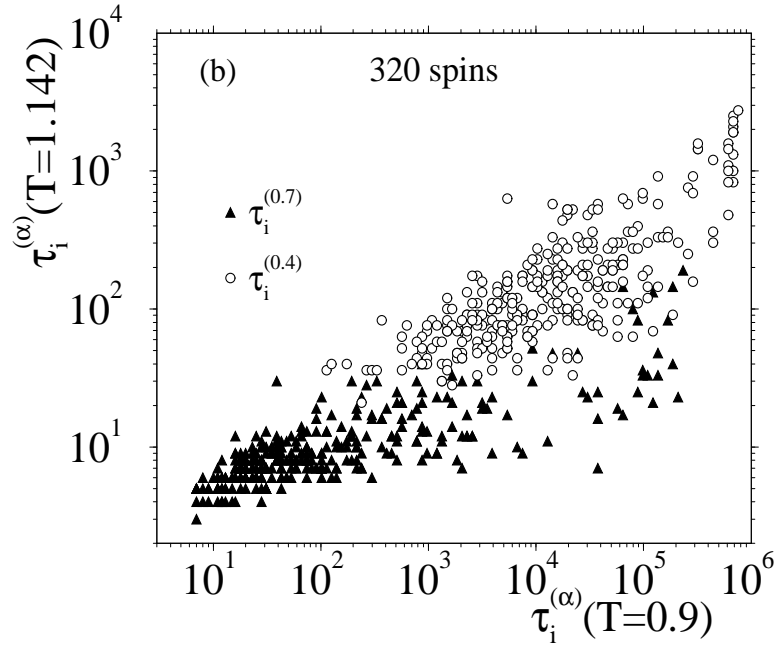


FIG. 17. a) Plot of $\tau_i^{(0.7)}$ [defined by $C_i(t = \tau_i) = 0.7$] versus $\tau_i^{(0.4)}$ [defined by $C_i(t = \tau_i) = 0.4$], for $T = 0.9$ and $T = 1.142$ (open and filled symbols, respectively) showing that the two relaxation times are correlated. Each point correspond to a different spin. b) Plot of the relaxation times $\tau_i^{(0.4)}$ and $\tau_i^{(0.7)}$ at $T = 1.142$ versus these relaxation times at $T = 0.9$. Each point correspond to a different spin.

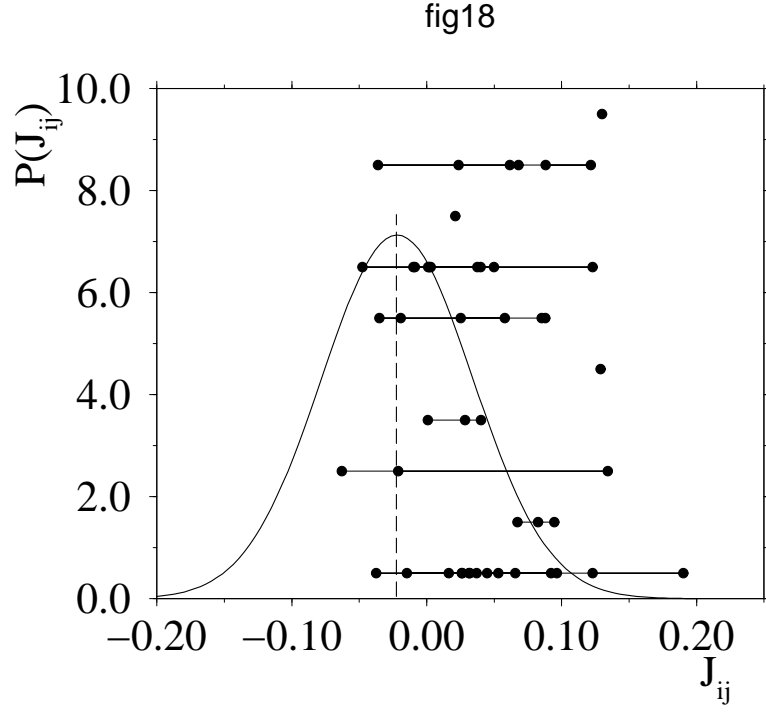


FIG. 18. Values of the bonds between spins with very slow relaxation in 10 different disorder realizations for 320 spins at a temperature $T = 0.9$ (filled circles). For clarity the points have been displaced vertically by various amounts. The continuous curve shows the Gaussian distribution from which the J_{ij} are extracted and the vertical dashed line shows its mean.